Reprinted from
Economic Geology
Vol. 72, 1977, pp. 804-826

An Analysis of the Cooling of Intrusives by Ground-Water Convection which Includes Boiling

L. M. CATHLES

Abstract

A finite difference model of the cooling of an igneous intrusive of limited volume is developed and used to investigate the relation between igneous intrusion, the formation of liquid and vapor dominated geothermal systems, and the formation of porphyry-type ore deposits. The model takes into account the properties of pure water and accommodates the phenomena of boiling and condensation. Permeability, level of intrusion, and pluton volume are systematically varied. Pressure, temperature, and fluid velocity are computed as functions of time.

It is found that a self-supported, vapor dominated steam zone is commonly (but briefly) formed above the intrusive. Condensed water bounds the steam zone above, and if the hydrothermal solutions are saline, a zone of boiling bounds the steam zone below. For pure water condensation is far more important than boiling—the solutions circulate around the critical point of water to become gaseous without boiling. Despite large temperature variations, convection causes fluid pressures throughout the whole uniform permeability system to be close to normal cold-water hydrostatic values. Thus, even in an active convecting system with moderate permeability variations, fluid pressure will tend toward normal hydrostatic values. Fluid circulation appears easily sufficient to produce a typical porphyry copper ore shell, but base metal precipitation probably must be controlled by mechanisms other than simple temperature drop.

Introduction

At the present time considerable effort is being directed toward exploitation of geothermal resources. Geothermal systems are thought to be associated somehow with magmatic intrusion. There has been considerable, highly illuminating modeling of geothermal systems such as Wairakei. However the modeling done to this point ignores the geometric details of the causative intrusive (which are usually poorly known), taking as a starting point a hot surface at depth (Mercer et al., 1975; Elder, 1965, 1966; Donaldson 1962). The temperature of the surface is steadily maintained so the models are steady state and do not evolve with time by themselves, although Mercer et al. have considered transient effects attending man's exploitation of the Wairakei geothermal area.

Geothermal systems have been classified as "vapor or liquid dominated" (White et al., 1971) and geologic examples of both types have been documented. Although it is generally felt an intrusive system may evolve from vapor dominated to wet in some cases, this intuition has not been refined into a formal model.

Finally there has been considerable discussion of the relation between mineral deposits (particularly porphyry copper deposits but also some nickel deposits) and intrusives, and the role ground-water convection may play in the alteration of certain intrusives and in the localization of ore near those intrusives (Sheppard et al., 1971; Norton, 1972; Cheney, 1974; Fyfe and Henley, 1973; Henley, 1973; Phillips, 1973; Whitney, 1975). Further quantification of these ideas may be possible.

Consideration of how an igneous pluton of limited volume may be expected to cool through conduction and ground-water convection provides useful insight into the relation between igneous intrusion, the formation of liquid and vapor dominated geothermal systems, and the formation of porphyry-type ore deposits. The main purpose of this paper is to present the results of model computations that bear on these connections.

The model developed accounts for convective cooling of the pluton by ground-water convection, takes into account the properties of (pure) water, and accounts for the thermal effects of fluid boiling and condensation. These factors are all shown to be important if the cooling history of an igneous intrusion is to be realistically estimated; of course boiling is vital to the investigation of the relation of vapor dominated and wet geothermal systems. The pluton is of limited dimensions, so the system evolves with time in a quasi-steady-state fashion until the initial thermal anomaly is erased.

The pluton is considered to intrude suddenly (at 700°C) into a water-saturated, fractured formation

of uniform permeability and normal geothermal gradient. The pluton permeability is taken to be the same as the intruded formation from the start. No consideration is given as to how fractures develop in the intrusive (a problem considered by Lister, 1974) or of how magmatic water of high salinity may exolve from the pluton (a problem elegantly considered by Whitney, 1975). Our focus is entirely on those convective processes that will occur after the pluton has developed throughgoing fractures and thus is permeable. The cases presented are deliberately kept as simple as possible so that fundamental features are clearly revealed. Complications can be added "in the mind's eye" once the general features are understood.

The model gas reservoirs are self-supported in the sense that cooler surrounding water will not cause them to collapse (Elder, 1966, p. 36 ff). "Steaming ground" may exist at shallow depths above the overlying condensed (water) zone. No account is taken of steaming ground phenomena, whose main effect would be to increase drastically the effective thermal conductivity of the region above the steaming ground water table. This deficiency is unimportant when free flow out the top surface (hot-spring activity) is permitted. The gas pressures of the model steam reservoirs closely follow the normal hydrostatic gradient and are therefore (at depths >500 m) substantially greater than the 32 to 38 bars observed by White et al. (1971) at depths up to 3,000 m at Geysers, California. Geysers is probably a steaming ground situation of perhaps unusual depth extent (otherwise a cold water head would have collapsed the vapor system as Elder has argued).

The greatest defect in the models presented is the assumption of constant salinity. Magmatic waters exolving from the intrusive can have salinities of 3 to 4 wt percent or greater (Whitney, 1975; Kilinc and Burnham, 1972). This salinity anomaly will be dispersed by the convective flow of water through the intrusive in a manner similar to the convective dispersal of the heat anomaly associated with the pluton. By extending the critical curve, salinity permits boiling at greater depths. Salinity strongly affects the ability of hydrothermal solutions to carry minerals. A proper account of geothermal systems and mineral deposition phenomena must include the effects of salinity on boiling and the dispersal of initially high magmatic salinities by fluid convection. The salinity problem is not directly treated in this paper, although insight as to its effects is gained from the calculations presented and their discussion.

In the next section the theoretical foundations necessary to describe convection of pure water (including boiling) in a fractured rock environment are given. Account is taken of the temperature and pressure dependence of viscosity, density, and enthalpy. The resulting mass, momentum, and energy balance equation are solved by standard finite difference methods (Alternating Direction Implicit) on a computer. In following sections several "heuristic" calculations of geological interest are presented and discussed.

Mathematical Formulation and Method of Solution [1]

The mathematical formulation and methods of solution are similar to those published previously by others. Only a brief, general review will be given.

Basically the model simply conserves mass, momentum, and energy:

$$\underline{\nabla}\cdot\underline{q} = 0 \quad \text{mass balance} \tag{1}$$

$$\underline{\nabla}\cdot\frac{\nu}{k'}\nabla\psi_x - g_0\frac{\partial\rho}{\partial y} = 0 \quad \text{momentum balance} \tag{2}$$

$$\rho_m(R + c_m)\frac{\partial T}{\partial t} = A - \underline{\nabla}\cdot\underline{q}\gamma T + K_m\nabla^2 T \quad \text{energy balance} \tag{3}$$

In addition, fluid pressure is given everywhere by the integral of Darcy's Law:

$$p(z) = p_s + g_0\int_s^s \rho dz + \int_z^s \frac{\nu}{k'} q_z dz \tag{4}$$

The only new feature is that the fluid properties of density, ρ, viscosity, ν, and pseudoheat capacity, γ, are treated as functions of pressure and temperature and looked up in tables appropriate for pure water (see Fig. 1). Values of pressure and temperature halfway through any particular computational timestep are used.

This methodology allows us to account for the unusual properties of water and the effects of boiling and condensation. If the usual approximation for density were taken, $\rho = \rho_0(1 - \alpha T)$, where α is a constant coefficient of thermal expansion, ν and γ were taken to be constant, and $R = 0$, equations (1) through (3) would reduce to the equations given by Holst and Aziz (1972) and Donaldson (1962, 1968). These authors assume $\underline{\nabla}\cdot q = 0$ as we do here. The equations would also be quite similar to those given by Palm et al. (1972), Elder (1967), Lapwood (1948), and Rubin (1973), who assumed $\underline{\nabla}\cdot\underline{V} = 0$ and therefore that ρ = constants everywhere except in the buoyant terms of the momentum equation. The method of numerical solution we have used is described by Carnahan et al. (1969, p. 452 ff).

[1] All symbols are defined in Appendix I.

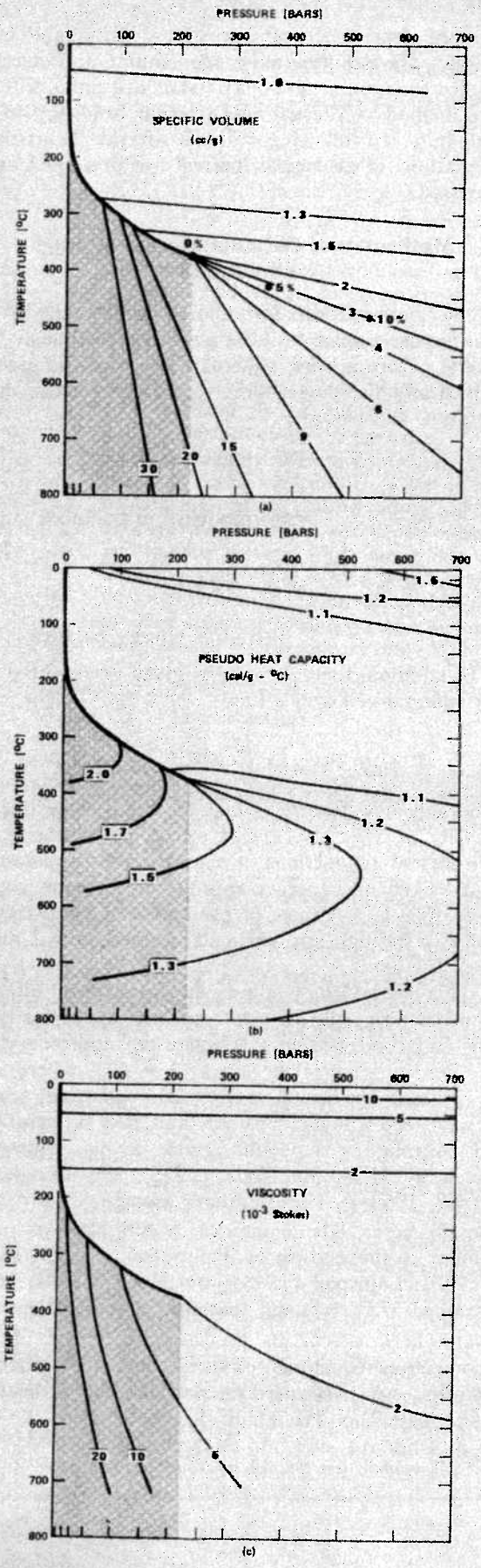

Since the treatment of boiling and condensation is novel, some further discussion might be useful. How the method of computation takes into account the heats of vaporization and condensation is best understood with reference to Figure 1b and equation (3). Suppose a packet of water is convecting upward across the critical curve in the region where γ would go from near 2 to near 1 cal/gm-°C. This crossing would occur near 300°C and 100 bars. Remembering T must be continuous across small distances, we see from (3) that the advection term, $\nabla \cdot q\ \gamma T$ equals $(\gamma^- - \gamma^+)\ qT\ (\Delta x \Delta y / \Delta x \Delta y \Delta z)$. Since $\gamma^- - \gamma^+ \simeq 1$ cal/gm = °C, we see the advection term accounts for a latent heat of condensation of ~300 cal/gm. The mass flux into the area $\Delta x \Delta y$ is q gm/cm², and the volume heated by the resulting release of latent heat is $\Delta x \Delta y \Delta z$.

Thus we see the advection term, together with the data shown in Figure 1b, automatically accounts for the latent heats of vaporization and condensation. The direction of fluid motion distinguishes condensation from vaporization.

It should be stressed that the method used *assumes* that only one fluid phase (liquid or gas) is present in any given spatial volume. Boiling or condensation occur at a surface in space. The mass flux of liquid up to the base of that surface exactly equals the mass flux of steam out the top, so fluid mass is neither created nor destroyed and equation (1) is satisfied.

Of course liquid and vapor could coexist if pressure and temperature varied in such a fashion as to follow the two-phase curve of water for some distance. Thus the assumption that liquid and vapor do not coexist over an appreciable volume is equivalent to assuming that p-T variations along a streamline do not follow the two-phase curve of water (along which liquid and gas can coexist) for any appreciable distance. The results of computations

FIG. 1a. The two-phase curve for pure water is shown with isopleths of constant specific volume. The shading indicates the region on the high-temperature side of the critical curve and corresponds to shading in the figures illustrating the convective cooling of plutons. The manner in which salinity extends the critical curve is shown by percentages indicating where the end of the critical curve would be for fluids of various wt percent NaCl. The data is from Sourirajan and Kennedy (1962). Pressure and temperature values stored in tables for access by the computer programs are indicated by tick marks on the top and left border of the diagram. Values between were obtained by linear extrapolation from table entries. Tick marks are at p = 1, 10, 25, 50, 100, 150, 200, 250, 300, 400, 500, 700, 1,000 bars; T = 20, 50, 100, 150, 200, 250, 300, 350, 400, 450, 500, 550, 600, 650, 700, 800°C.

FIG. 1b. Two two-phase curve for pure water is shown with isopleths of pseudoheat capacity (γ). Pseudoheat capacity is obtained by dividing the enthalpy at various temperatures and pressures by the temperature. Data are from tables 3 and 4 of Keenan et al. (1969). Shading and tick marks are as in Figure 1a.

FIG. 1c. The two-phase curve of pure water is shown with isopleths of viscosity (millistokes). The shading and tick marks are as in Figure 1a. Data is from table 8 of Keenen et al. (1969) and Bruges et al. (1966).

show that in general the streamline p-T curves intersect the critical curve of water at high angles (see Fig. 6). Thus the critical curve is crossed cleanly and the assumption of a sharp boundary between gas and liquid is appropriate.

Other details of the model that were considered during its formulation are summarized below:

1. Flow through a fractured igneous formation is described by Darcy's Law. Darcy's Law applies to flow through fractures or joints as well as flow through the pores in a sandstone and remains valid for flow rates three orders of magnitude greater than considered in this paper (for likely formation conditions). We assume there is no lower limit to the validity of Darcy's Law.

2. For a localized heat source such as would be produced by an igneous intrusive, convection will occur providing only that the intruded formation is permeable and water saturated. No critical temperature gradient (Rayleigh number) need be exceeded. The geometry of the heat source will drive forced convection not free convection. The rate of convection and the amount of fluid circulated through the intrusive will be controlled by the permeability of the intrusive and intruded formation as well as by the size, initial temperature, and location of the intrusive.

3. It is implicitly assumed that the fractures or joints through which hydrothermal solutions convect are less than 200 m apart. Provided this is true the interiors of the "matrix block" between fractures can track changes in hydrothermal solution temperature closely enough to remain essentially in thermal equilibrium with the fluid—in accord with an assumption made in modeling.

4. Heat generated by alteration reactions which occur as the convecting fluids interact with and cool the pluton are accounted for through R in equation (3). It is assumed that over the entire cooling history of the pluton 36 calories are generated in this way per gram of intrusive. This appears to be a reasonable estimate (Fyfe, 1974; Norton and Cathles, in press). For the sake of consistency it is assumed such exothermic chemical reactions occur even when the permeability is zero and the intrusive cools entirely by conduction.

5. Pressure is computed by integrating Darcy's equation and assuming the pressure at the surface is constant and known. It may be preferable to assume the pressure at some considerable depth is known (e.g., is unperturbed). If this convention is adopted the pressure contours will be altered as discussed in the last section.

6. Instabilities arise from the advection term which is given an improved treatment (Torrance, 1968, Method V) which preserves causality (heat anomalies are advected only downstream), conserves energy, and introduces only slight false conduction.

7. A variable grid spacing is used so that high surface heat flows such as are observed in geothermal areas may be accommodated. Most calculations were done on a 19×29 point grid.

8. Boundary conditions are written in general terms so free solution flow out the top surface can be modeled as well as the situation where no flow out the top surface is permitted. Temperature boundary conditions (insulating or fixed temperature) can also be freely specified. In Figures 2 and 3 no flow, insulating boundary conditions apply to the right and left boundaries. The base is no flow with a heat flux of 1.5 HFU (so long as the geothermal gradient is normal; near the pluton, while the pluton and its immediate environment was hot, the heat flux was taken to be zero), and the top is either no flow or free flow with a fixed temperature of 20°C.

9. The accuracy of computation is checked by inventorying the heat remaining in the computation domain, verifying that losses are accounted for by heat fluxes out of the domain and by checking that computations with denser point spacing give results similar to those with less dense spacing (e.g., computations converge).

10. Model computations give the total heat flux out the top surface. For the cases where no flow out the top surface is permitted this heat flux is all conductive. In the case where free solution flow out the top surface is permitted interpretation of the proportion of heat transported across the surface by hot-spring activity through intermittent fractures and by conduction is allowed. The models presented define only the total top surface heat flux.

11. Placing the model intrusive in the middle of the computation domain gives very similar results to placing the pluton at the bottom of the domain but at the same depth. The geometry chosen for the computation domain does not appear to distort significantly the results obtained.

Results of Computations

Results of computations are given in Figures 2 through 11. Figure 2 shows the thermal evolution of a pluton 0.75 km in half-width and 2.25 km high, whose top is 2.75 km beneath the surface. The figure shows the thermal and fluid flow evolution of a system, assuming the formation and pluton permeabilities are 0, 0.05, and 0.25 millidarcies (md). In all cases the cooling of the pluton is considered to produce exothermic chemical reactions which generate, over the full course of cooling, 36 calories per gram of pluton. This is small compared to the amount of heat available from cooling, which is ap-

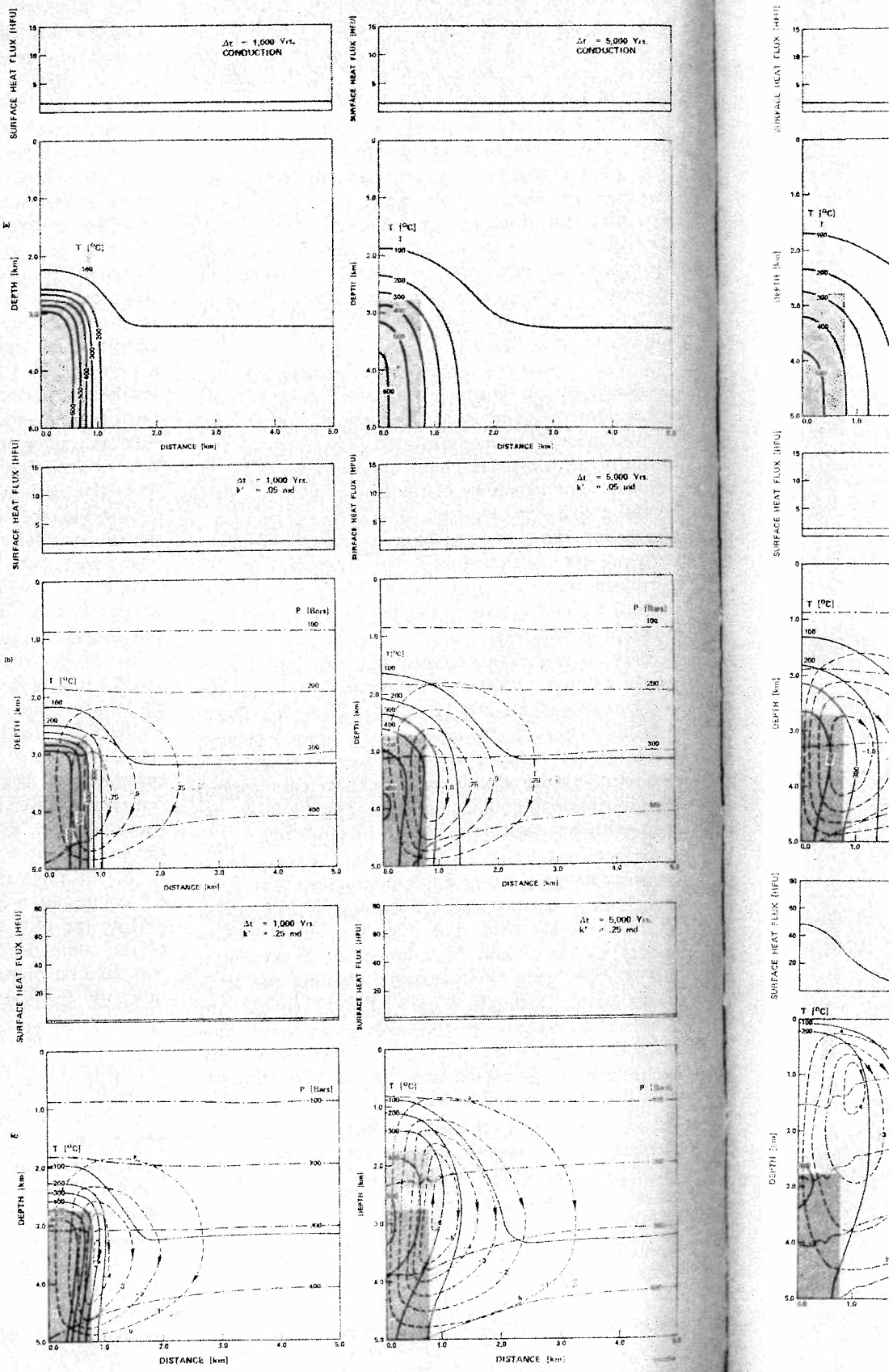

FIG. 2. Cooling histories for uniform 0-, 0.05-, and 0.25-md formation (and intrusive) permeabilities. In each figure temperature is indicated by isotherms (solid lines), pressure is indicated by isobars (dot dashed lines), and flow is indicated by stream lines (dashed lines). Pressure contours are computed using equation (4) and assuming the top surface pressure is 10 bars. The normalized stream function, $\bar{\psi}$, is related to the mass flux rate as indicated in Appendix I. At the top of each figure the total surface heat flux is given. In cases (such as this figure) where the top surface is impermeable to solution flow, the heat flux out the top surface is entirely conducive. Differences in cooling history as a function of permeability are apparent. In the permeable 0.25-md case, the thermal anomaly initially associated with the intrusive rises like a hot-air balloon until it impinges on the surface. The temperature contours near the base of the pluton are pinched in. This mode of cooling is quite different from the conductive case, where the isotherms spread out symmetrically in all directions from the intrusive. Hydrostatic pressure contours are quite flat in all cases until the thermal anomaly reaches the near-surface environment. The rate of fluid circulation (given by the curl of the stream function, and approximately by the difference between the minimum in the stream function and 0) increases almost linearly with permeability (see Fig. 8a). The shaded areas in (c) above the intrusive (which is also shaded) are regions that lie on the high-temperature side of the critical curve of water. These regions correspond to similarly shaded regions in Figures 1 and 6. The top portion of the shaded zone is a zone of stream condensation. This can be seen by comparing the letters on the $\bar{\psi} = -1$ streamline of (c) at 5,000 years with the p-T loop corresponding to this streamline in Figure 6a. The conventions of Figure 3 are the same as described here.

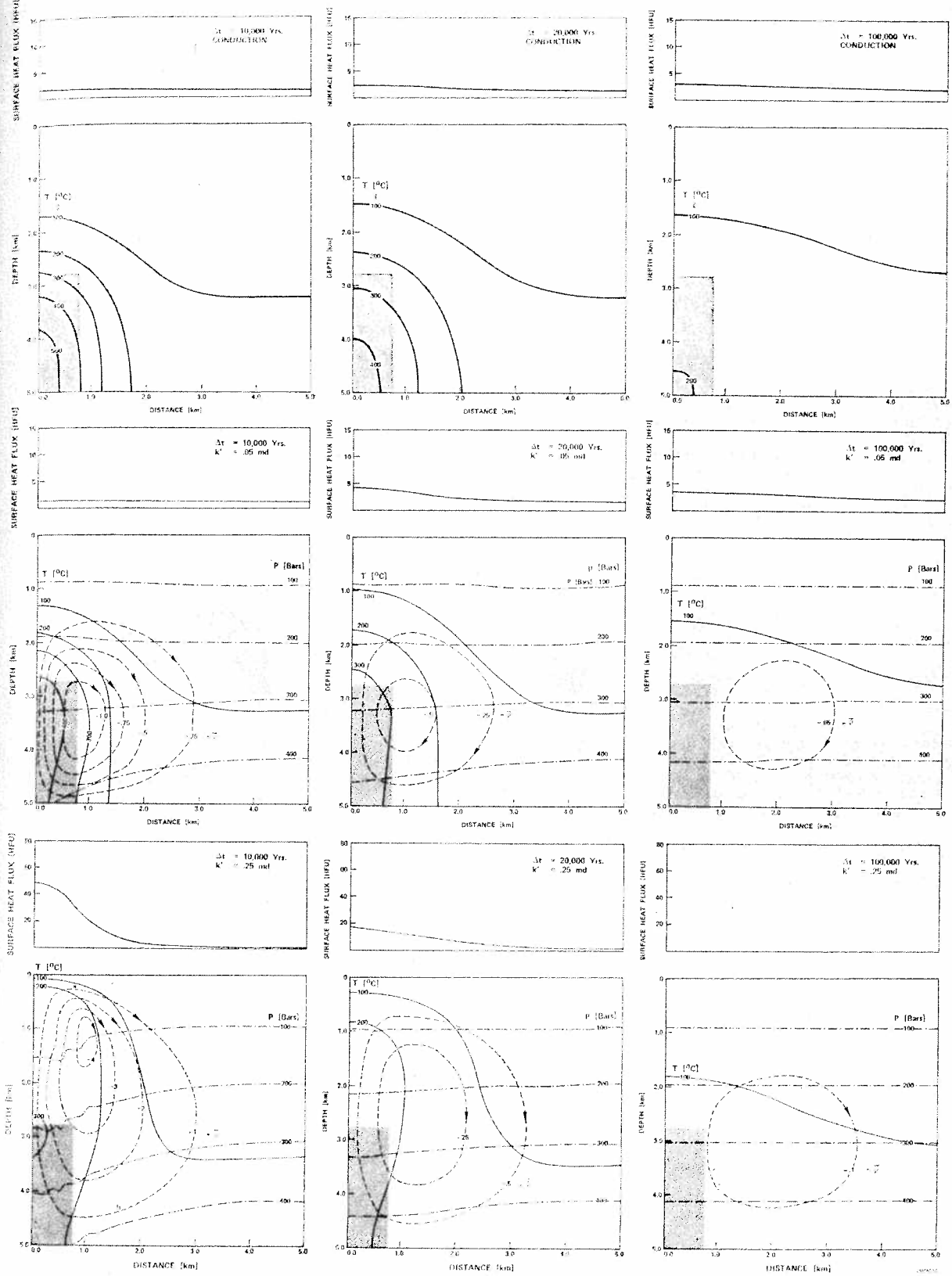
SURFACE HEAT FLUX (HFU)
Δt = 10,000 Yrs.
CONDUCTION
Δt = 20,000 Yrs.
CONDUCTION
Δt = 100,000 Yrs.
CONDUCTION
T [°C]
DEPTH [km]
DISTANCE [km]
Δt = 10,000 Yrs.
k' = .05 md
Δt = 20,000 Yrs.
k' = .05 md
Δt = 100,000 Yrs.
k' = .05 md
P [Bars]
Δt = 10,000 Yrs.
k' = .25 md
Δt = 20,000 Yrs.
k' = .25 md
Δt = 100,000 Yrs.
k' = .25 md

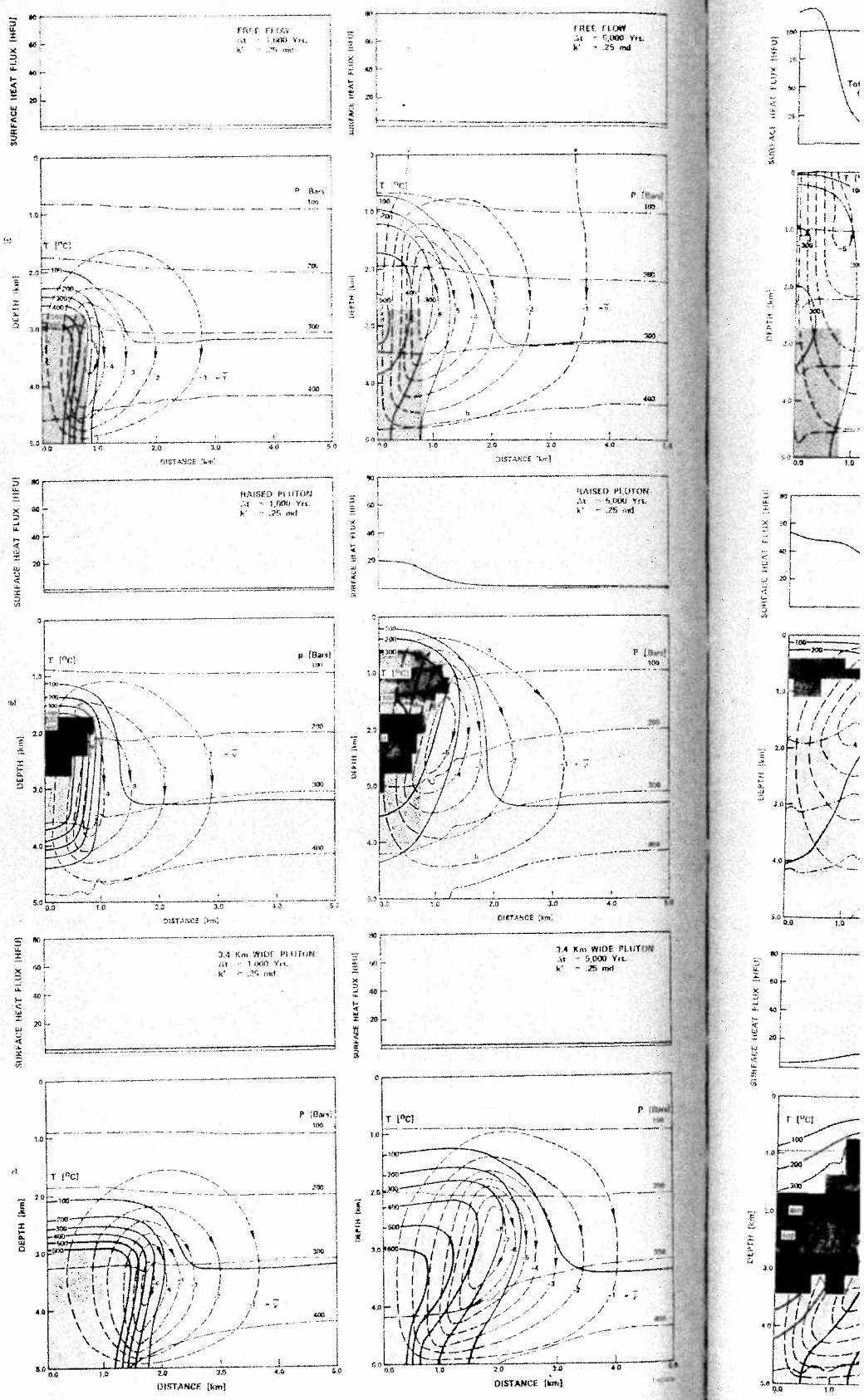

FIG. 3. The effects of free flow out the top surface, decreasing the burial depth and increasing the pluton width, are illustrated for a formation (and intrusive) permeability of 0.25 md. These cases are typical of the larger numbers of cases analyzed in Figure 9. It can be seen that if free flow out the top surface is permitted, the isobars remain flat even after the heat anomaly has reached the near surface. Also far higher surface heat fluxes are permitted. As discussed in the text, in case of free surface flow, surface heat flux may be interpreted as partly due to hot-spring activity and partly due to conductive heat transport. If the depth of burial is decreased the heat flow anomaly reaches the surface faster. If the pluton width is increased a broader surface heat anomaly results and a Bénard cell type of convection is initiated over the top of the pluton [(c) at 20,000 years]. As in Figure 2 the shaded regions above the pluton are those whose fluids lie on the high-temperature side of the two-phase curve of water and thus might be called vapor dominated. The shading of these zones corresponds to the shading in Figure 1.

proximately 600°C × 0.2 cal/g°C × 2.7 g/cc or 324/g of stock cooled.

The permeabilities 0.05 to 0.5 md are chosen to be representative of the low range of permeabilities in fractured igneous rock and the range over which convective heat transport becomes important and then dominates conductive heat transport. The permeability of crystalline rock at the Los Alamos hot-rock test site in the Jemez Mountains, New Mexico, is estimated to be about 0.002 md (Aamodt, 1976). Permeabilities of ocean-ridge basalt have been estimated at 0.45 md (Ribando et al., 1976); permeabilities in Wairakei's Waiora aquifier have been taken to be about 100 md (Mercer et al., 1975; Elder 1966).

Pure conductive cooling (Fig. 2a) of the pluton never produces a significant surface heat flow anomaly. The maximum surface heat flow occurs 65,000 years after intrusion and is only 3.4 HFU (compared to a "normal" heat flux of 1.5 HFU). The pluton cools symmetrically; the isotherms extend further from the base of the pluton than from the top of the pluton because they are superimposed on a normal geothermal gradient. The temperature of the top portion of the pluton steadily drops from a temperature of about 400°C at 1,000 years after intrusion.

If the formation permeability is 0.05 md (Fig. 2b), convective dissipation cools the intrusive more rapidly and causes the isotherms to bulge out over the top of the intrusive and pinch in near the base. The temperature of the top of the pluton remains at about 400°C for the first 10,000 years of cooling and then decreases in temperature only because the temperature of the entire pluton has dropped below 400°C. A maximum surface heat flow of 4.9 HFU occurs directly over the center of the pluton 35,000 years after intrusion.

In a formation of 0.25-md permeability, the effects of fluid flow in pinching in the isotherms at the base and ballooning them out at the top are even more apparent. The shaded area above the pluton indicates the region which lies on the high-temperature side of the critical curve (the shaded regions in Fig. 1). This area is a region of "steam" which, if discovered during its short lifetime, might be a valuable geothermal resource. The vapor dominated steam region occurs largely before the intrusive event is detectable by high heat flows at the surface. The maximum surface heat flow of 47 HFU occurs 10,000 years after intrusion. The region just above the pluton heats up to over 500°C and then cools down.

If the same pluton cools in a formation of permeability 0.5 md, the maximum heat flow anomaly is 69 HFU and occurs 6,500 years after intrusion. The convective rise of the thermal anomaly is even more obvious than in the 0.25-md case and the surface expression of high heat flow occurs more quickly.

Figure 3 illustrates various changes on the base 0.25-md case shown in Figure 2c. If free flow out the top surface is permitted (hot-spring activity) much higher surface heat fluxes result. The maximum surface heat flow is 170 HFU 7,750 years after intrusion compared to 47 HFU 10,000 years after intrusion for the no flow case. If intrusion reaches shallower levels, the areas of vapor are larger than in the base case due to lower hydrostatic pressures and the surface heat flow is manifested sooner because the surface is closer to the intrusive. The fluid circulation is slightly less because vapor has a higher viscosity than liquid. The streamlines tend to avoid the shaded vapor zone. Finally increasing pluton half-width to 1.7 km causes convection to concentrate at the edge of the intrusive and produce a heat flow which is a maximum over the edge of the pluton rather than over the center. Because the pluton contains more heat, high temperatures can be carried to shallower depths and the vapor zone is larger. Secondary circulation cells develop after the temperature contours have been up-bowed at the edges of the intrusions. A "Rayleigh-Bénard" cell pattern is thus developed for plutons whose total width (not half-width) is comparable to the depth to the pluton.

The rate of fluid circulation can be calculated from the streamlines at any time and the total amount of fluid circulation that has occurred from the time of intrusion can be determined. Figure 4 shows the total amount of fluid that has circulated through various cases illustrated in Figures 2 and 3. In a formation with permeability of 0.05 md, 90 kg of water circulate through each sq cm of the top central portion of the intrusive in the 100,000 year cooling time computed. For a permeability of 0.25 md this figure is 250 kg per sq cm, and for a formation permeability of 0.5 md, the figure is 300 kg, per sq cm. As discussed later, the amount of fluid circulation does not go up linearily with permeability because the amount of heat in the initial thermal anomaly is limited. It can be seen that for wide plutons the maximum fluid circulation may not be in the intrusive or centrally located with respect to the pluton.

Figure 5 illustrates the fluid properties over the 200-year step between 4,800 and 5,000 years after intrusion for the 0.25-md domain shown in Figure 2. Significant variations in specific volume, psuedo-heat capacity, and viscosity are indicated. The high specific volume of the fluid above the intrusive provides the buoyant force to drive convection. The

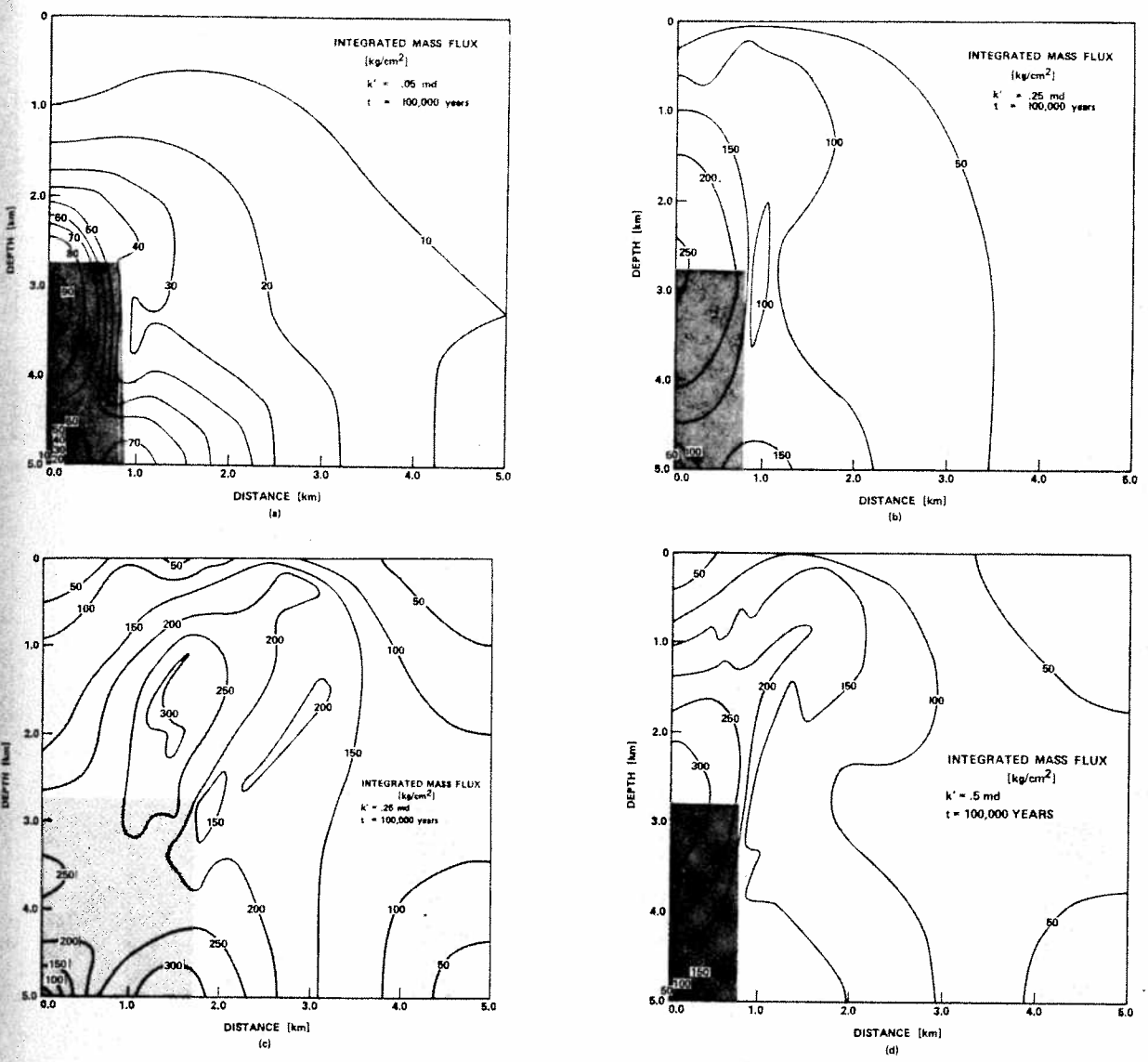

FIG. 4. The total amount of hydrothermal solution passing through each centimeter squared of surface area over 100,000 years of cooling is shown for various formation permeabilities and pluton geometries. As shown in Figures 8 and 9 this integrated mass flux is strongly dependent on permeability and pluton volume. It can be seen that for wide plutons the regions of maximum integrated mass flux are not necessarily centrally located inside the intrusive.

maximum specific volume is quite a bit larger than would be indicated by approximations usually used (specific volume $= 1/(\rho_0 - .001\ \rho_0 T) = 1.67$ for $T = 400°C$). Variations in pseudoheat capacity show condensation will dump a significant amount of heat above the boiling zone, as the ability of the hydrothermal fluids to carry heat decreases. Variations in viscosity show a large region where the viscosity is nearly one-fifth its value at the surface. In this region, convection is five times easier than it would be if the viscosity of the fluid were constant. A high viscosity zone associated with the vapor dominated area is also indicated (viscosity of the fluid increases as the fluid becomes gaslike).

Figure 5d shows the magnitude of fluid mass flux at 5,000 years after intrusion. The maximum mass flux rate can be seen to be about 15 g/cm²-yr. That is, across the right-hand top of the pluton, about 15 grams of water will circulate on average through each sq cm surface area perpendicular to the direction of the flow in one year.

Figure 6 shows the pressure and temperature conditions encountered by fluid as it circulates around streamlines shown in Figures 2 and 3. The figure is

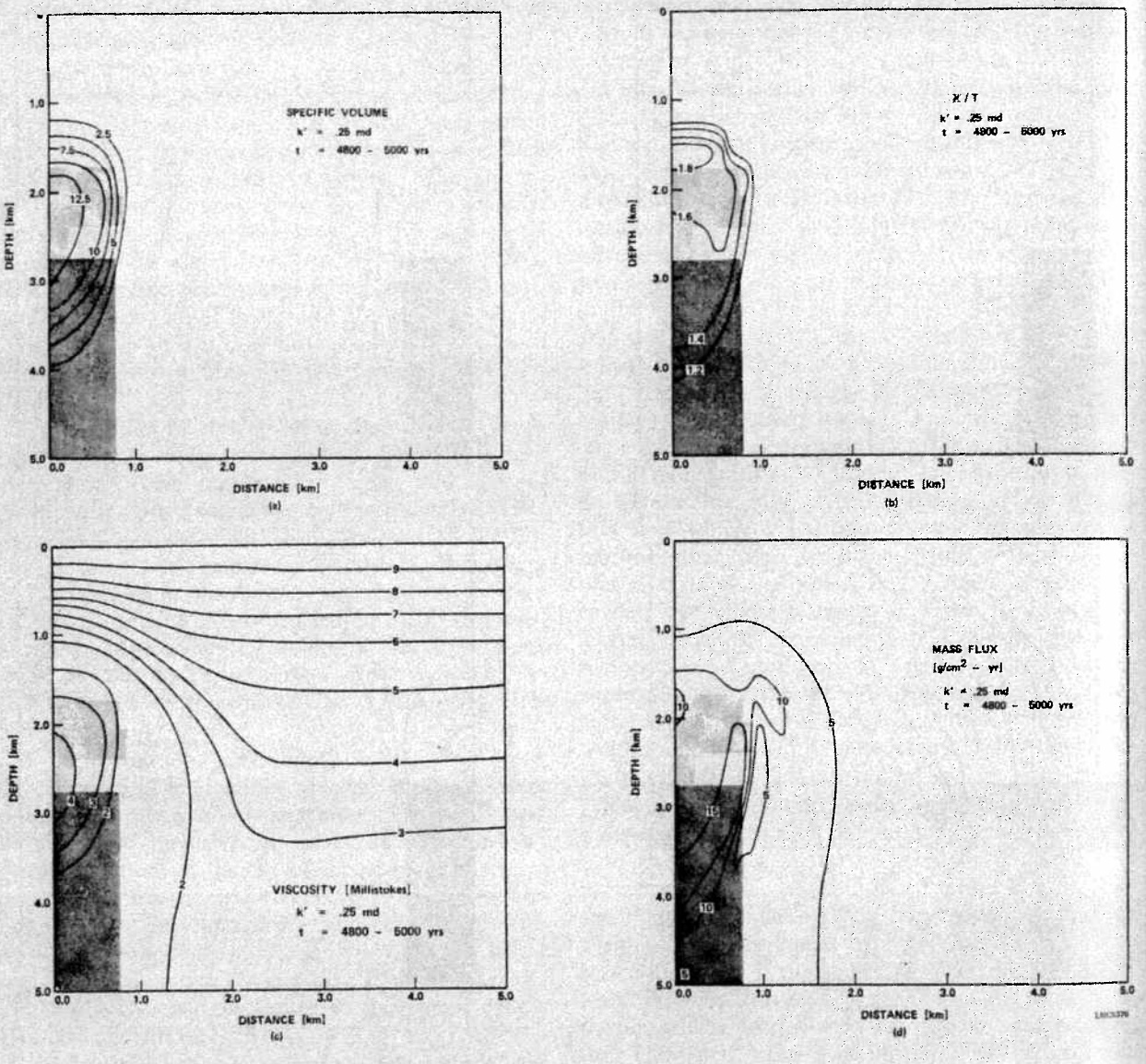

FIG. 5. Fluid properties are shown for the case of Figure 2c 4,800 to 5,000 years after intrusion. As commented in the text the combination of large specific volumes and reduced viscosity produce convection about six times faster than constant parameters models. The steep gradient in pseudoheat capacity ($\mathcal{H}/T$) strongly accelerates the upward migration of the intrusive's thermal anomaly. Fluid circulation rates are 10 to 15 g/cm² yearly.

arranged so that the circulation sense is the same as in Figures 2 and 3. The p-T curves may also be superimposed on the plots in Figure 1 to show the variations in specific volume, pseudoheat capacity, and viscosity along the streamlines. The fluid circulation loops rise toward lower pressures and involve increasingly smaller excursions in temperature as the pluton cools. The loops cross the critical curve from the gas to the liquid side. The solution becomes gaseous by circulating around the end of the two-phase curve. For pure water condensation is therefore a much more important phenomena than boiling. The curves cut the two-phase curve of water at a sharp angle confirming our assumption that liquid and vapor will not coexist in the same rock volume. The return solutions follow the normal geothermal gradient as one might expect.

Figures 7, 8, 9, and 10 indicate the systematics of varying permeability, pluton burial depth, pluton half-width, and the boundary conditions for flow at the top surface. The main effect of permeability (Fig. 7a) and the convection it permits is to decrease the maximum temperature of the domain more rapidly than would be possible by conduction. The

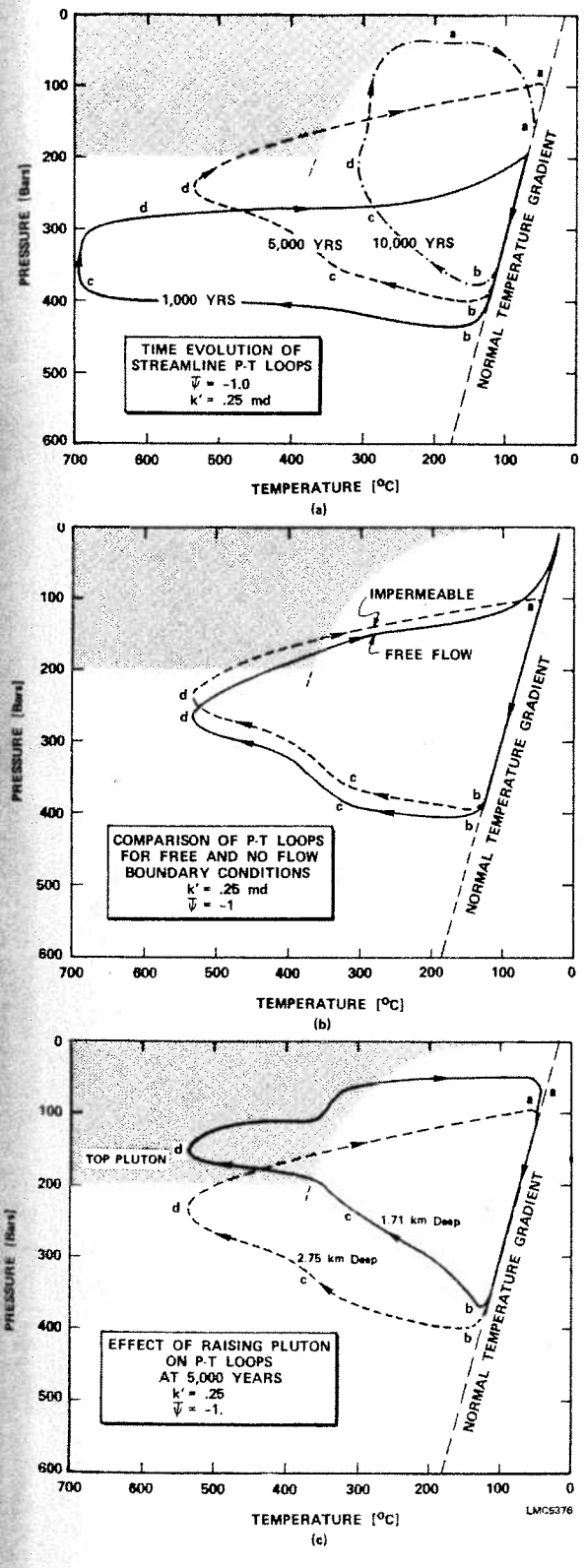

FIG. 6. The variation in pressure and temperature around selected streamlines in Figures 2 and 3. The letters key to corresponding letters in those figures. The first figure (a) refers to curves in Figure 2c. The second figure refers to streamlines in Figure 3a (solid) and 2c (dotted), both 5,000 years after intrusion. Figure (c) refers to streamlines in Figure 3b (solid) and Figure 2c (dotted). The curves indicate that solutions increase rapidly in temperature at nearly constant pressure as they circulate into a pluton and decrease strongly in temperature again at nearly constant pressure upon leaving the top of the pluton. The solutions increase in temperature along the normal geothermal gradient as they circulate downward to enter the base of the intrusive. It can be seen that the flow paths cut the critical curve of water at a sharp angle; thus fluids are either liquid or gaseous and not a mixture of liquid and gas. For pure water condensation is a far more important phenomenon than boiling, which occurs only in (c). As commented in the text however, if the solution had only 10 wt percent salinity, boiling as well as condensation would occur in most of the cases shown. Salinity extends the critical curve of water (see Fig. 1a) to about 500 bars, so the p-T curves would cross the salinity-extended two-phase curve both as temperature increased and as temperature decreased. Free solution flow out the surface has only a small effect on the pressure and temperature conditions encountered around the $\bar{\psi} = -1$ streamline (b), and decreasing the depth of intrusive burial decreases the pressure encountered around the streamline loop as one might expect (c).

most important effects are realized in the early stages of cooling when large buoyant forces exist to drive the most rapid fluid circulation. Higher permeabilities permit higher maximum surface heat fluxes (Fig. 7c).

The maximum rate of fluid circulation is linearly proportional to permeability (Fig. 8a). Surface heat flow does not increase in such a simple way but increases sharply over a critical range of permeability between about 0.1 and 0.3 md (Fig. 8c). The maximum integrated mass flux (shown for particular cases in Fig. 4) also increases with permeability at a decreasing rate.

The last effects may be understood as follows: If the pluton were maintained at constant temperature, increasing the permeability would lead to a directly proportional increase in solution circulation rate, the integrated amount of circulation over any given time, and the surface heat flux. The last proportionality is not obvious but has been shown to be the case for Rayleigh-Bénard convection (Elder, 1967) and would also be the case for the situation just hypothesized. The pluton is not maintained at constant temperature, however, but decreases in temperature with time. The amount of fluid circulation that is possible therefore depends not only on the permeability but also on the length of time required to cool the initial intrusion. Increases in the rate of fluid circulation are canceled to a certain extent by the shorter time required to cool the intrusive by the greater circulation. Similarly, although faster circulation rates move the thermal anomaly to the surface with less loss of heat, there is still an unavoidable loss associated with the requirement of heating the rock above the intrusive. Higher permeabilities can pro-

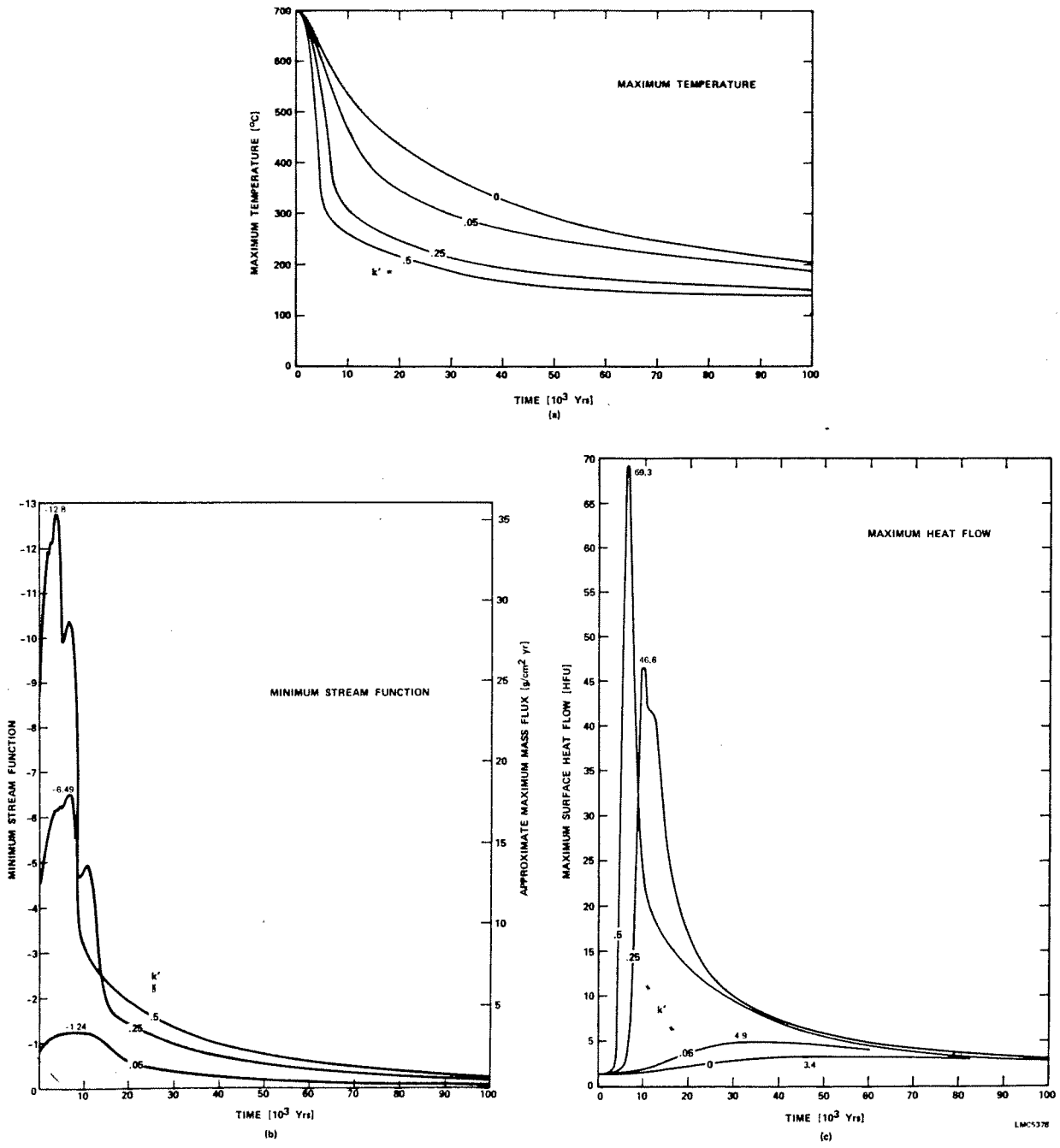

FIG. 7. The effects of permeability on cooling rate, solution circulation rate, and maximum surface heat flow. The convection allowed in permeable water-saturated formations permits a far more rapid cooling than would be allowed by conduction alone. The very steep decline in the $k' = 0.5$- and 0.25-md cases results from the additional cooling permitted by variable enthalpy. Most of the solution flow occurs in the first 10,000 to 20,000 years of cooling. The small secondary maxima in (b) results from the increase in the permeability that follows the disappearance of steam dominated zones. The maximum circulation rate and permeability are linearly related as indicated in Figure 8a. Maximum surface heat flow also increases as permeability increases but not proportionately (see Fig. 8c). By comparing (b) and (c) it can be seen that most of the intense fluid circulation is finished by the time strong surface heat fluxes are manifested.

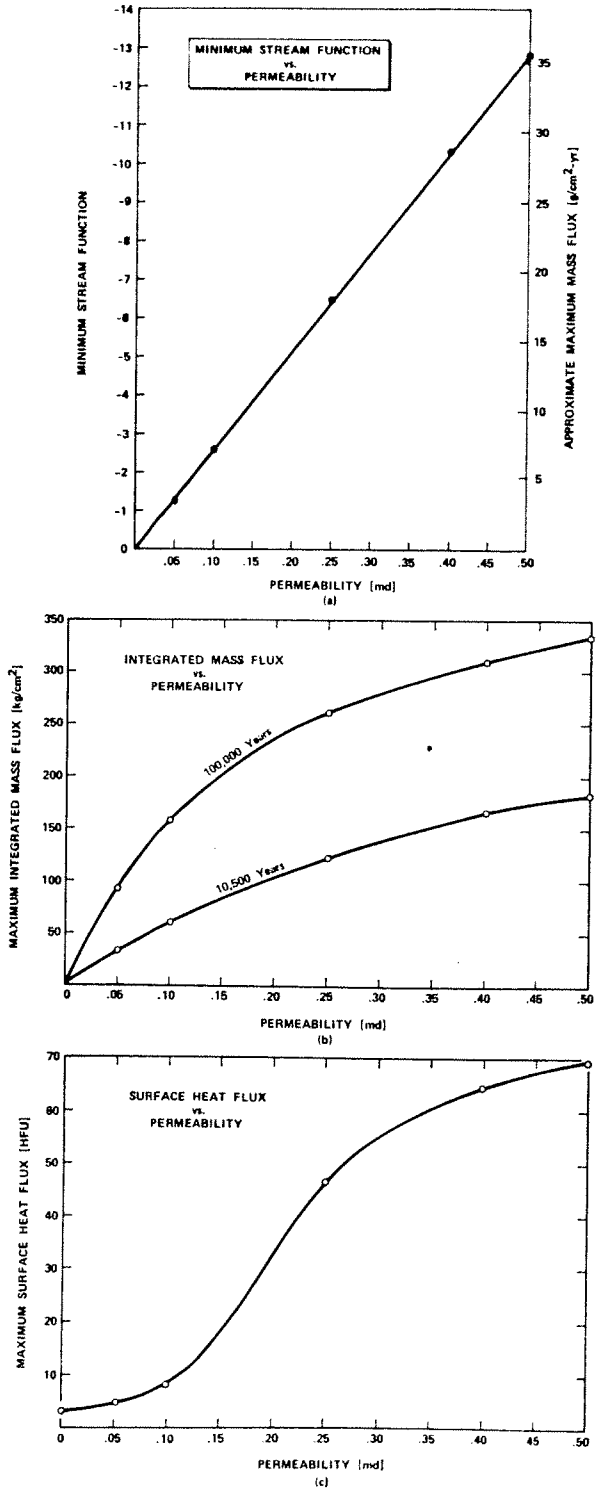

FIG. 8. The dependence of minimum stream function (approximate maximum mass flux), integrated mass flux, and maximum surface heat flux on permeability. The minimum stream function is linearly proportional to permeability. As discussed in the text, heat flow and integrated mass flux would also be linearly related to permeability if it were not for the finite heat contents of the pluton.

mote a narrower plumelike upwelling, but the constriction of the upwelling plume does not proceed rapidly enough to promote a proportional relationship between permeability and maximum surface heat flow.

Increasing the pluton half-width increases the maximum rate of fluid circulation only slightly (Fig. 9a). Similarly, as remarked previously, decreasing the depth of burial decreases the rate of fluid circulation slightly, probably as a result of the increased amount of space dominated by higher viscosity steam. The decrease for 0.05-md formation permeabilities is less noticeable than for 0.25-md formation permeabilities since substantially less volume is occupied by steam in the 0.05-md case (Fig. 9b).

The total amount of solution circulating through the pluton increases almost linearly with pluton half-width (Fig. 9c). Convection can continue longer if the initial intrusive contains more thermal energy. The increase in the duration of high surface heat flow is only about half as great as would have been expected on the basis of the increase in pluton size, however (Fig. 10a). Increasing the pluton half-width from 0.75 to 1.17 km represents a 56 percent increase in pluton volume, but the duration of 30 HFU surface heat flow is increased only 21 percent (from 5,700 to 6,900 years). Similarly, the increase from 0.75 to 1.70 km half-width increases the pluton volume by 127 percent but the duration of 30 HFU surface heat flux is increased only 68 percent. The explanation for this discrepancy is that high surface heat flows occur over a larger surface area for the wider plutons.

Allowing free solution flow out the top surface has little effect on the rate of fluid circulation (Fig. 9b) but has a very substantial effect on the total heat flux at the surface (Fig. 9f). In the 0.25-md case the maximum surface heat flux is almost quadrupled by allowing free solution flow. A substantial effect is also seen for the 0.05-md case. Even low permeability formations can produce large surface heat flow anomalies if flow out the surface occurs and intrusion reaches shallow depths (Fig. 10b).

The maximum surface heat flux increases as the depth of burial decreases for low permeability domains but is nearly independent of pluton burial depth for higher permeability domains (Fig. 9f). For the higher permeability domains, the decrease in overburden that must heated is canceled by the decrease in solution flow rates caused by the more gaseous nature of the fluid at shallower depths.

Figure 11 illustrates the importance of taking accurate representations of fluid viscosity, specific volume, and enthalpy. Variable fluid density and viscosity allow circulation to occur much more easily. If condensation and boiling are *not* permitted, com-

puted results are similar to computations using the usual Bousinesq approximations [$\rho = \rho_0(1 - \alpha T)$, ν = constant] *provided* the formation permeability is six times greater. Condensation greatly facilitates the upward migration of the heat anomaly and allows the intrusive to cool far more rapidly. Taking account of variable fluid properties makes a very substantial difference in computed results.

Geological Implications

Fluid pressure in a convecting system

It is often of interest to know the hydrostatic or fluid pressure as a function of depth in a hydrothermal system. For example, such knowledge may be used to make a pressure correction to fluid inclusion filling temperatures. It is argued below, on the basis of the simple calculations made, that the increase in pressure with depth in a hydrothermal system may be quite close to the normal hydrostatic pressure gradient of 100 bars per kilometer, provided the permeability is reasonably uniform. This conclusion requires some interpretation of the figures given in the previous section, since in those figures the surface pressure was arbitrarily assumed to be constant and of a known value (in this case 10 bars).

Figures 2 and 3 show that in most cases the computed isobars are quite flat. In these cases a uniform normal hydrostatic gradient is indicated directly. The hydrostatic gradient is the same in the cool portions of the computation domain as it is in the hot igneous pluton. Fluid flow has compensated for the much lower fluid densities near the pluton, the resistance to upward flow increasing the pressure to normal levels.

In those cases where the thermal anomaly has reached the near surface, however, the equal pressure contours are bent downward. The reason is that near the surface the upward migration of solutions cannot occur to the extent necessary to flatten the pressure contours. In the case where free solution flow out the top is permitted (Fig. 3a), however, the pressure contours remain flat even when the thermal anomaly reaches the surface. Notice that in the cases where the pressure contours are bent downward, all of the deeper pressure contours are bent downward a nearly identical amount. Apparently the pressure perturbations originating in the near-surface environment will persist downward indefinitely.

Persistance of pressure perturbations to infinite depths is not physically reasonable, and some reinterpretation of the assumptions by which pressure is calculated in these cases is indicated. As discussed in the previous section, we assume that the surface pressure is fixed and constant. This is entirely reasonable in the case where free solution flow out the surface is permitted. In this case, the pressure at the surface could be 1 bar (1 atm) or greater if the surface lay under a shallow layer of water (e.g., 10 bars). However, in the case of zero surface solution flow, maintenance of a constant surface pressure is less realistic. If the geological situation is that of a ground-water table, the ground-water table may rise in response to fluid convection. Thus, at the level which we choose to call the "surface" the pressure may change with time due to the weight of overlying pore fluids (e.g., the elevated water table). In these cases, a more reasonable convention might be that the pressure at some large depth remain constant. This will be certainly true at sufficiently large depths. In this case the deeper pressure contours would be flattened and the pressure contour at the surface ($z = 0$) would be up-bowed. In the cases of Figures 2 and 3 discussed before, this would mean an exchange of all the down-bowed pressure contours for a single up-bowed surface pressure contour whose physical interpretation would be an up-doming of the ground-water table. Since the pressure contours in Figures 2c and 3b and c are depressed about 100 bars, the up-doming of the ground-water table would be 1 km or more (more as the fluid density falls below 1 g/cc).

Since ground-water tables commonly die at depths less than 1 km, up-bowing of the ground-water table as suggested by the cases considered would cause free solution flow out the top surface. In this case, of course, the pressure contours would be flat, as indicated in Figure 3a.

Figure 12 shows pressure gradients through the axis of the pluton for some of the cases in Figures 2 and 3 and shows how solution flow reduces, and in the free flow case nearly eliminates, deviations from a normal hydrostatic pressure gradients. To reiterate: It is suggested that the pressures at the right-hand end of the curves in Figure 12 should be made coincident, whereupon deviations from normal hydrostatic pressures occur near the surface and are

FIG. 9. The dependence of minimum stream function, integrated mass flux, and maximum surface heat flow on pluton half-width and burial depth. Fluid circulation is not strongly affected by either pluton half-width or depth of burial. Integrated mass flux increases as the depth of pluton burial increases for high permeabilities. Less volume is occupied by high viscosity steam with deeper burial, and deeper burial allows larger convection cells. Integrated mass flux is nearly proportional to pluton half-widths (i.e., to the total amount of thermal energy in the initial intrusive). Free flow out the top surface does not significantly affect the rate of fluid circulation but dramatically increases the maximum surface heat flux.

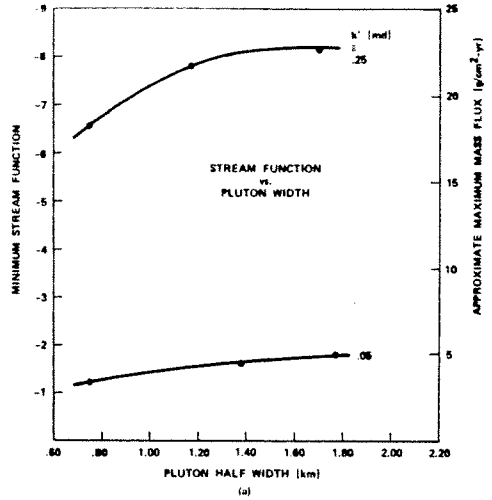
STREAM FUNCTION
vs.
PLUTON WIDTH
k' [md]
.25
.05
MINIMUM STREAM FUNCTION
APPROXIMATE MAXIMUM MASS FLUX [g/cm²-yr]
PLUTON HALF WIDTH [km]
(a)

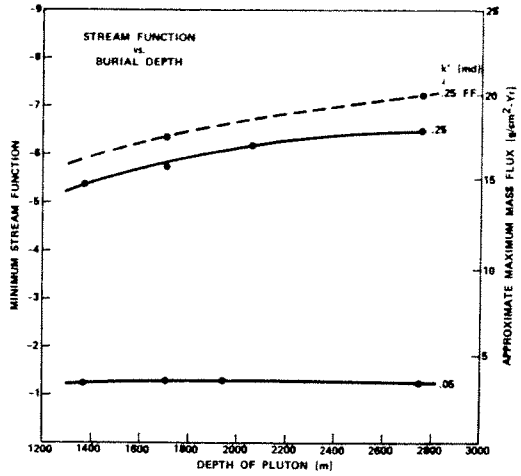
STREAM FUNCTION
vs.
BURIAL DEPTH
k' [md]
.25 FF
.25
.05
MINIMUM STREAM FUNCTION
APPROXIMATE MAXIMUM MASS FLUX [g/cm²-Yr]
DEPTH OF PLUTON [m]

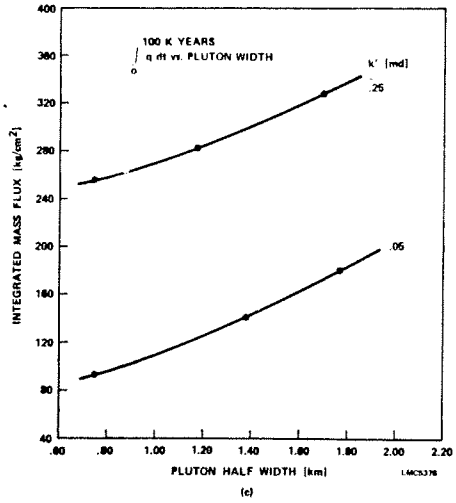
100 K YEARS
∫ q dt vs. PLUTON WIDTH
k' [md]
.25
.05
INTEGRATED MASS FLUX [kg/cm²]
PLUTON HALF WIDTH [km]
(c)

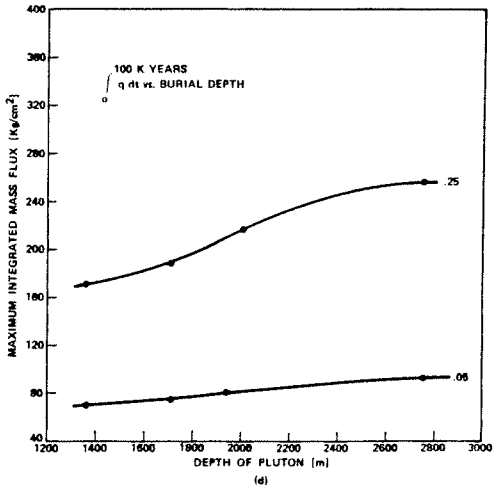
100 K YEARS
∫ q dt vs. BURIAL DEPTH
.25
.05
MAXIMUM INTEGRATED MASS FLUX [Kg/cm²]
DEPTH OF PLUTON [m]
(d)

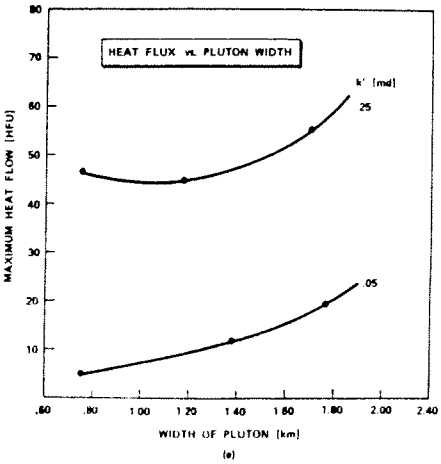
HEAT FLUX vs. PLUTON WIDTH
k' [md]
.25
.05
MAXIMUM HEAT FLOW [HFU]
WIDTH OF PLUTON [km]
(e)

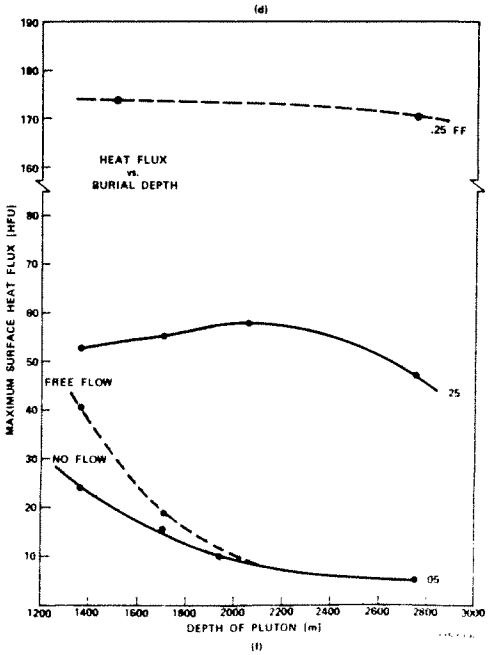
.25 FF
HEAT FLUX
vs.
BURIAL DEPTH
FREE FLOW
NO FLOW
.25
.05
MAXIMUM SURFACE HEAT FLUX [HFU]
DEPTH OF PLUTON [m]
(f)

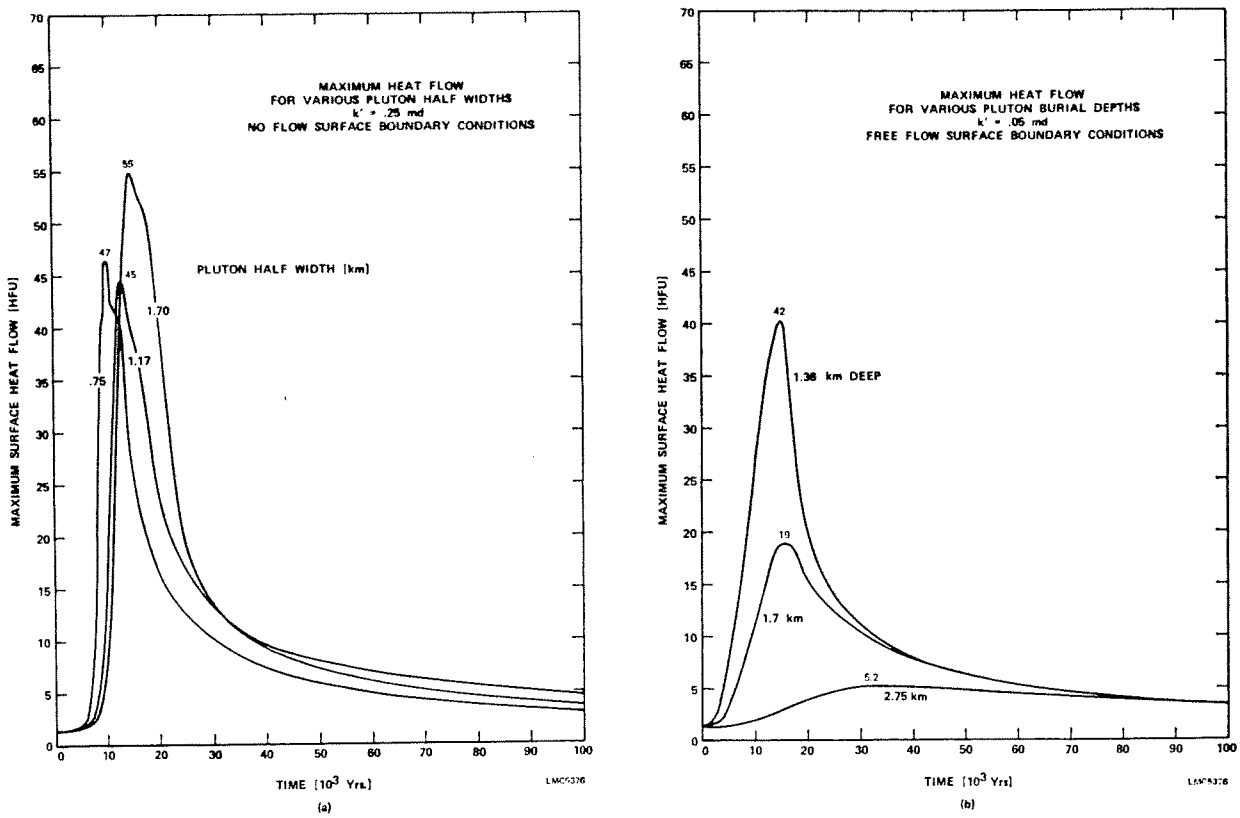

FIG. 10. Dependence of surface heat flux on pluton half-width and depth of burial. As discussed in the text wider plutons do not increase the duration of high surface heat flow proportionately because the regions of high surface heat flow are broader (see Fig. 3c). Even low permeability formations can produce significant surface heat flow anomalies if free solution flow out the top surface is permitted and if the depth of pluton burial is small.

caused by an up-bowing of the ground-water table. Computationally assuming constant pressure at great depth gives this result directly.

We conclude that for a uniformly permeable formation, pressure contours will be flat and normal hydrostatic pressure gradients may be applied to actively convecting hydrothermal systems as well as to normal cool, static ground water.

These results apply only to formations with reasonably uniform permeabilities. It is easy to imagine cases of nonuniform permeability where the fluid pressure profile would not be normal hydrostatic (e.g., flow upward through a high permeability zone with a low permeability top—most of the pressure drop would occur in the low permeability cap). Some variation in permeability can be tolerated, however, because the fluid viscosity varies by about a factor of five in different parts of the computation domain (see Fig. 5c). Even in a formation with moderate variations in permeability the results here suggest hydrostatic gradients will tend to be more normal than not.

Implications for geothermal resource formation

The consequences of the modeling presented for geothermal energy are relatively straightforward. Small plutons can generate large surface heat fluxes and substantial reservoirs of hot rock and even steam or vapor dominated reservoirs (i.e., regions which lie on the high-temperature side of the critical curve of water). The model heat fluxes are comparable to the average heat flux at Wairakei, for example, which, according to Elder (1965) is 50 HFU over an area 50 sq km with local heat fluxes up to 10^4 HFU. However, it is clear that the duration of the high surface heat fluxes (see Figs. 7c and 10a) are of short duration, generally less than 20,000 years. It can be seen from Figures 2 and 3 that the lifetimes of the vapor dominated regions are shorter still, generally less than 5,000 to 10,000 years.

Ten or even 20,000 years is geologically a very short period of time. It is unlikely that there are many conventionally exploitable intrusions of sufficiently recent vintage to have hydrothermal systems of the type modeled associated with them at the pres-

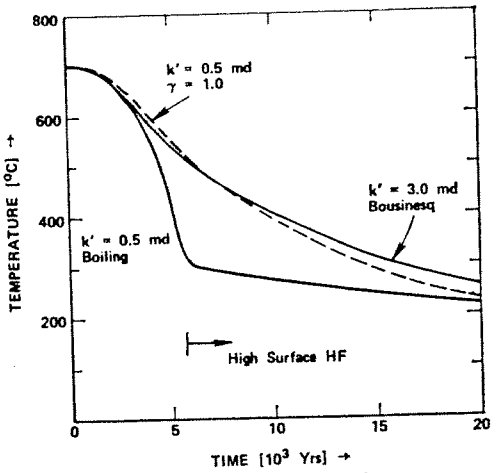

FIG. 11. The importance of taking fluid properties into account is illustrated by the differences in maximum temperature versus time. With a constant pseudoheat capacity of 1 cal/g-°C, variable fluid viscosity and density produce a cooling history similar to constant viscosity and density models with a formation permeability six times larger (dashed curve). Latent heats of condensation allow faster upward migration of the thermal anomaly and thus substantially more rapid cooling. The abrupt change of shape of this curve occurs when the heat anomaly's upward migration is arrested by the top surface. No flow out the top is permitted in this case.

ent geological instant. Permeabilities of at least 0.25 md would be required for economic flows of steam into producing wells. Unless intrusives substantially larger than 3 km in diameter are envisioned, exploration for geothermal energy would thus apparently best be devoted to areas where intrusion is thought to go on continuously, e.g., at actively rifting areas such as Wairakei, New Zealand, or near historically active volcanic systems.

For single isolated intrusives, Figures 2 and 3 suggest that the best geothermal systems may lie beneath surfaces which have yet to manifest high heat fluxes. By the time the strongest manifestation of surface heat flow occurs in the models, the vapor dominated regions have shrunk considerably in size and much of the most valuable thermal energy may have been dissipated.

Implications for porphyry-type copper deposit formation

Crerar and Barnes (1976) have shown experimentally that three important factors affecting copper solubility in hydrothermal solutions are temperature, salinity, and pH. Copper concentrations in solution of 1 gram per liter or greater are possible at temperatures of 350°C and high salinity. Changes in copper concentration of an order of magnitude (1 g/l to 100 ppm) result from changes in temperature from 350° to 250°C or from changes in salinity from 5.8 to 0.58 wt percent, or from changes in acidity from pH 3 to pH 4 (Crerar and Barnes, 1976). The models presented in the last section permit quantification of the conditions under which low-grade copper originally in the intrusive may be concentrated in a higher grade ore shell draped around the intrusive.

For a 0.4 wt percent copper cutoff, ore shells of porphyry copper deposits are typically 180 to 240 m (600 to 800 feet) thick (Lowell and Guilbert, 1970, p. 385). It is not certain the ore shell curls over the top of the intrusive with which it is associated, although this occurs in some cases (James, 1971). Typically 70 percent of the ore lies in the causative intrusive, but there are many cases where mineralization lies mostly (~80%) outside the causative intrusive (Lowell and Guilbert, 1970).

By area ratio it is quite possible to form a model ore shell 200 m thick and 1 km long draped over the model intrusive having a grade of 0.43 wt percent copper by scavenging or collecting 0.05 wt percent copper from the intrusive. The intrusive dimensions are 0.75 by 2.25 km so the area ratio is 0.75 × 2.25

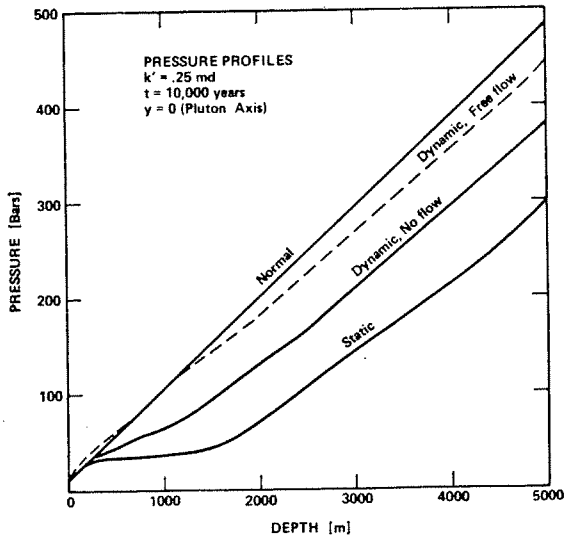

FIG. 12. Pressure as a function of depth down the pluton axis (y = 0) is compared to the normal hydrostatic pressure increase. The curve labeled "static" indicates the increase in pressure with depth in Figure 2c due to fluid mass only. Fluid flow increases this pressure to the curve labeled "dynamic; no flow" (also from Fig. 2c but with both terms in equation (4) contributing, not just the fluid mass term). Fluid circulation reduces the deviation in hydrostatic pressure from "normal" by about a factor of two. The curve marked "dynamic; free flow" is the axial pressure from Figure 3a and shows that if free solution flow out the top surface is permitted perturbations of hydrostatic pressure from normal are nearly eliminated by fluid flow. It is suggested in the text that the "dynamic; no-flow" curve should actually be superimposed on the "normal" curve over most of its length with the perturbations toward abnormally high pressures at depths less than 1,000 meters being caused by an up-bowing of the ground-water table.

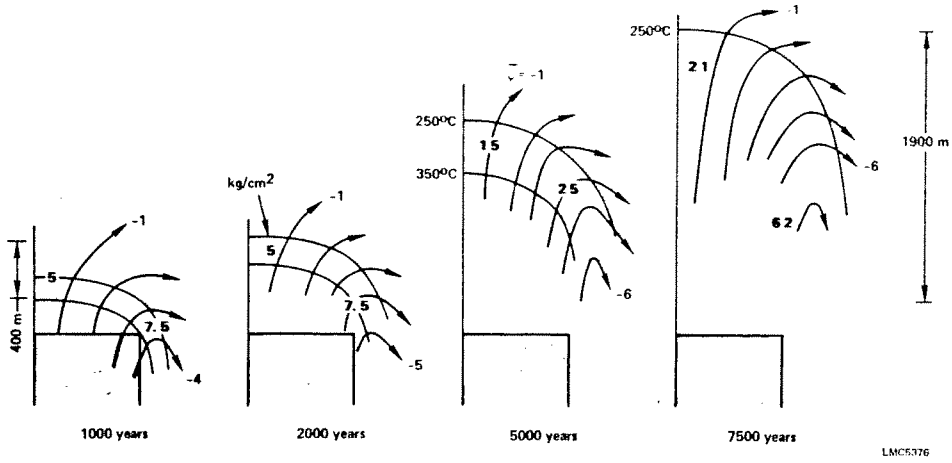

FIG. 13. The region between 250° and 350°C through which upwelling solutions flow in the case of Figure 2c is shown as a function of time. The stream lines of Figure 2c are sketched and the direction of flow indicated by arrows. The numbers between the two bounding temperature lines show the mass flux that occurs through this temperature domain over the interval of time from the last diagram. For example between 1,000 and 2,000 years 5 kg/cm² have circulated through the 250° to 350°C temperature zone immediately above the center of the pluton. As discussed in the text this figure shows that a narrow ore shell probably cannot be produced by the temperature dependence of copper solubility alone. By the time sufficient integrated solution flow has occurred to produce an ore zone similar to those observed, the critical temperature range has changed position and become too smeared out to produce a narrow ore shell.

divided by 0.2 × 1.0, which is equal to 8.44; 8.44 × 0.05 = 0.42 wt percent. With a 1 g copper per kg water drop in solution copper concentration per pass through the ore zone, 216 kg solution is required per sq cm surface area of ore shell to form the deposit. Figures 4 and 8 show such solution fluxes are easily obtained for formation permeabilities of 0.25 md or greater. The problem, therefore, is to find a mechanism for precipitating the intrusive copper in a narrow ore shell.

One possibility is to use the temperature gradient at the top of the pluton during the early stages of intrusive cooling. Figure 13 shows that the region between 350° and 250°C forms a suitable ore shell during the first 2,000 years or so of pluton cooling. After ~2,000 years, the temperature region becomes too broad to produce a narrow ore shell or provide a relatively large concentration factor.

Unfortunately, the amount of fluid circulated through the ore shell in the first 2,000 years of cooling is too small to account for the necessary copper precipitation. For the 0.25-md case shown in Figure 13, at most about 15 kg of solution have circulated through each sq cm of surface area of the hypothesized ore shell. With a change in copper concentration of 1 g per kg, this means that at most 15 g of copper can be precipitated per sq cm of ore shell; the grade of the ore shell can at most be about 0.028 wt percent copper (equals 15 g Cu divided by 200 × 10^2 cm × 2.7 g/cc).

Of course, if the formation were more permeable, more fluid might flow through the ore shell in the early stages of pluton cooling. Using the linear relationship between initial flow rate and permeability (see Fig. 8a), the 0.028 wt percent ore shell might be increased to 0.4 wt percent if the domain permeability were 3.5 md instead of 0.25 md. It seems unlikely, however, that 216 kg per sq cm water, the amount required to pass through the ore shell in order to produce the 0.4 wt percent grade with a 1 g Cu per kg H_2O drop per pass, could circulate through the intrusive without very substantially dispersing the initial heat anomaly. After all, the thermal anomaly is pretty well erased in 100,000 years at which time the integrated mass flux is at most only 250 kg per sq cm (see Figs. 2c and 4b). 216 kg water per sq cm will certainly smear out temperature gradients sufficiently to make thermal deposition in a 400-m shell difficult. It seems unlikely that temperature gradients alone can produce the type of porphyry ore shell commonly observed.[2]

As mentioned before, solution fluxes greater than required can be produced by small plutons if the formation permeability is greater than 0.25 md (Figs. 4 and 8b). Thus, there appears to be no problem

[2] If convection were prolonged strong temperature gradients could be maintained near the surface and substantial mineral deposition could occur there. This mechanism may well apply to kuroko-type deposits (Ohmoto and Rye, 1974). Porphyry copper ore shells are thought to have formed several kilometers beneath the surface, however.

precipitating an ore shell provided some nonthermal precipitation mechanism can be found. The best candidate is probably boiling.

The effect of salinity

Chlorine will be highly fractionated into the vapor phase as the intrusive solidifies (Kilinc and Burnham, 1972). One might therefore expect the salinity of magmatic water exsolved from the intrusive to be high. This is verified by high salinities found in fluid inclusions in many porphyry copper deposits. Salinities in fluid inclusion can be as high as 46 wt percent NaCl. (Moore and Nash, 1974; Roedder, 1971). Salinity, as previously mentioned, is an important factor affecting the ability of solution to transport copper and other base metals (Crerar and Barnes, 1976; Holland, 1972).

Although we have not explicitly taken salinity into account, several inferences are possible regarding the effects. If the intrusive initially contains magmatic waters of high salinity in addition to a heat anomaly, the salinity anomaly of the intrusive will be convected upward and dispersed in a manner similar to the way the thermal anomaly is carried upward and dispersed. There are several important differences, however.

First, unless there is surface discharge into a shallow, well-mixed sea or lake, salinity cannot escape out the top surface and will be recirculated into the surrounding formation. Low-salinity formation waters will dilute the salinity of the initial magmatic fluids, and the eventual result will be a formation at uniform temperature and salinity with the eventual salinity slightly higher than previously, reflecting the introduction of magmatic salt.

Secondly, and more importantly, if there is no boiling, the upward convection of the salt anomaly will proceed much faster than the upward convection of the thermal anomaly. This is basically because the convecting solutions can carry much more salt, relative to the ability of the formation to store salt, than they can carry heat, relative to the ability of the formaion to absorb heat.

For the case where advection (fluid transport) of heat and salinity is much more important than diffusion of heat or salinity (e.g., the permeability of the formation is greater than ~0.1 md), the upward migration rates of heat and salinity can be quantified. If the fluid mass flux is q g/cm²-yr, the upward migration of heat, V_z^{heat}, will just be:

$$V_z^{heat} = \frac{\text{heat flux [cal/cm}^2\text{-sec]}}{\text{heat storage capacity [cal/cm}^3\text{]}} = \frac{\Delta T \gamma q}{\Delta T \rho_m c_m} \text{ [cm/yr]}$$

Taking values in Appendix I, γ between 1 and 2 (Fig. 1b) and q = 15 g/cm²-yr, a value appropriate for the first 10,000 years of convection of a 0.25-md formation (see Fig. 7b),

$$V_z^{heat} = 0.28 \text{ to } 0.56 \text{ cm/yr}$$

The estimated time for the thermal anomaly in Figure 2c to reach the surface is therefore 2,750 m/(0.28 − 0.56) = 5,000 to 10,000 years. This is in good agreement with the computed initiation of high surface heat flows at about 8,000 years (Fig. 7c).

The upward migration of salinity will be given by

$$V_z^{salinity} = \frac{\text{salt flux [g NaCl/cm}^2\text{-sec]}}{\text{salt storage capacity g NaCl/cm}^3} = \frac{\Delta S q/\rho}{\Delta S \phi} \text{ [cm/yr]}$$

ΔS is the magmatic salinity minus the base level formation salinity and is measured in grams NaCl/cm³ of fluid. Thus,

$$\frac{V_z^{salinity}}{V_z^{heat}} = \frac{\gamma}{\phi \rho_m c_m \rho}$$

Since $1/\rho > 1.0$, and $\gamma/\rho_m c_m > 1.85$, and $\phi < .04$,

$$\frac{V_z^{salinity}}{V_z^{heat}} > 46.$$

The salt anomaly will migrate upward toward the surface at least 46 times *faster* than the associated heat anomaly!

This means regions above the intrusive should increase in pore solution salinity significantly before they increase much in temperature. In fact, the intrusive's salinity anomaly may be flushed out and dispersed before the intrusive has cooled very much. Since salinity is required to carry significant base metal concentrations in solution, this suggests mineral deposition occurs soon after intrusion, while the intrusive itself is still very hot.

A final effect of salinity is that it extends the critical curve of water and thus permits fluid boiling at much greater pressures and depths. If the hydrothermal solution in Figure 2c had just 10 percent salinity, *boiling* as well as condensation would take place (compare extension of critical curve indicated in Fig. 1a with p-T loops in Fig. 6a). In the presence of CO_2, boiling may significantly raise the solution pH and thereby cause base metal precipitation (H. Ohmoto, pers. commun.).

Since steam can carry less dissolved salt than condensed water, the boiling salinity permits will complicate the upward convective dispersion of salinity.

Conclusions

A finite difference model has been developed that accounts for the variable properties of pure water (viscosity, specific volume, and enthalpy) and can

accommodate the effects of boiling and condensation. Variable water properties are shown to affect significantly computational results and their inclusion is therefore of interest (Fig. 11). The model is applied to the cooling of igneous intrusives to gain insight on the origin of geothermal systems and porphyry-type copper mineralization.

It is found from the modeling presented in this paper that fluid convection has the effect of carrying the initial thermal anomaly upward off the intrusive (like a hot-air ballon) until it impinges on the surface (Fig. 2c). At this point strong surface geothermal activity begins and convection practically ceases. Although there is some overlap, the geothermal reservoir tends to be "disconnected" from the intrusive in time and space. Surface heat flow reflects the cooling of a near-surface pool of hot water that migrated at an earlier time from an intrusive at depth (Fig. 7c).

Permeability, depth of burial, and pluton volume were systematically varied to study their effect on pluton cooling. Cooling is dramatically accelerated as permeability is increased (Fig. 7a). The maximum fluid circulation rate increases proportionally with permeability (Figs. 7b and 8a). The total mass of fluid circulated through the pluton during cooling increases with permeability (not linearly) and pluton volume (nearly linearly). The maximum surface heat flux depends most strongly on whether or not free solution flow (hot-spring activity) occurs out the top surface (Fig. 9f). Surface heat flux also depends importantly on permeability (Fig. 8c), depth of pluton burial (Fig. 10b), and pluton volume (Fig. 9e).

Despite the fact fluid densities are drastically reduced by the higher temperatures near the pluton, the resulting fluid circulation causes the hydrostatic pressure profile to be nearly normal in the uniform permeability cases computed. Even for formations with moderately variable permeability, hydrostatic pressures should tend to be more normal than not, due to the effects of convection.

For pure water, consdensation is found to be a much more important phenomena than boiling. Hydrothermal solutions circulate around the critical point of water and hence become "gaseous" without boiling. Even for intrusives buried by 2.75 km of overburden, a vapor dominated reservoir is produced briefly beneath a condensed liquid zone for formation permeabilities $\sim$0.25 md or greater. This vapor dominated region is self-supporting in the sense hydrostatic pressures within it are as great as hydrostatic pressures outside (Fig. 3a). If the fluids were saline, boiling would occur at the base of the vapor dominated steam zone as well as condensation at its top (Fig. 6a).

The duration of intense geothermal activity caused by the model intrusives is brief (<20,000 years). Unless intrusives are much bigger than those considered here, exploration for geothermal reserves may best be directed toward areas of very recent (volcanic centers) or nearly continuous (Wairakei) intrusive activity. The best geothermal resources may be those which have yet to manifest strong surface heat flows.

The amount of fluid circulation near the intrusive is accounted and shown to be sufficient to produce a typical porphyry copper ore shell. The laboratory data of Crerar (1974) are assumed to be valid and it is assumed copper originates in the intrusive. With these assumptions the natural fluid convection can account for the redistribution of copper from a porphyry intrusive into an ore shell outside the intrusive in the surrounding country rock as is frequently observed. However, it is shown that temperature gradients alone probably cannot account for the ore location (Fig. 13). Other methods of precipitation such as salinity gradients, boiling, or wall-rock reactions must be appealed to.

If the fluids evolving from the intrusive are highly saline, the intrusive's initial salinity anomaly will be convected upward by the fluid circulation and dispersed just as the heat anomaly is convected upward and dispersed. The upward advection and dispersion of the salinity anomaly will be much faster than the upward advection and dispersion of the heat anomaly, however (probably about 50 times faster). Since high fluid salinities are required to maintain high base metal solution concentrations, the dispersion of salinity may play an important role in mineral deposition. Boiling may complicate salinity dispersion.

Acknowledgments

The author would like to thank Kennecott Copper Corporation for support of the research reported in part in this paper and for permission to publish the results. Geochemical and geological discussions with Dr. Denis Norton during the early part of this work while Denis was the Kennecott, and Denis' enthusiastic support of the work during that period, are also gratefully acknowledged.

LEDGEMONT LABORATORY
KENNECOTT COPPER CORPORATION
128 SPRING STREET
LEXINGTON, MASSACHUSETTS 02173
August 31, December 28, 1976

REFERENCES

Aamodt, R. L., 1976, Hydraulic fracturing in and communication between two adjacent wellbores [abs.]: Am. Geophys. Union Trans., v. 57, p. 349.

Bruges, E. A., Latto, B., and Kay, K., 1966, New correlations and tables of the coefficient of viscosity of water and

steam up to 1,000 bar and 1,000°C: Internat. Jour. Heat and Mass Transfer, v. 9, p. 465–480.
Burnham, C. W., and Davis, N. F., 1971, The role of water in silicone melts I. P-V-T relations in the system $NaAlSi_3O_8$-H_2O to 10 kilo-bars and 1,000°C: Am. Jour. Sci. v. 270, p. 54–79.
Burnham, C. W., Holloway, J. R., and Davis, N. F., 1969, Thermodynamic properties of water to 1,000°C and 1,000 bars: Geol. Soc. America Spec. Paper 132, p. 96.
Carnahan, B., Luther, H. A., and Wilkes, J. O., 1969, Applied numerical methods: New York, John Wiley & Sons, Inc., p. 604.
Carslaw, H. S., and Jaeger, J. C., 1959, Conduction of heat in solids: Oxford, Clarendon Press, p. 510.
Cathles, L. M., and Apps, J., 1975, A model of the dump leaching process that incorporates both physics and chemistry: Metallurgical Trans. v. 6B, p. 617–624.
Cathles, L. M., Spedden, H. R., and Malouf, E. E., 1974, Tracer technique to measure the diffusional accessibility of matrix block mineralization, *in* Aplan, F. F., McKinney, W. A., and Pernichele, A. D., eds., Solution mining symposium: New York, Am. Inst. Mining Metall. Petroleum Engineers, p. 129–147.
Cheney, E. S., 1974, Examples of the application of sulfur isotopes to economic geology: Am. Inst. Mining and Metall. Petroleum Engineers Trans., v. 255, p. 31–38.
Crerar, D. A., 1974, Solvation and deposition of chalcopyrite and chalcocite assemblages in hydrothermal solutions: Ph.D. thesis, Penn. State University, p. 164.
Crerar, D. A., and Barnes, H., 1976, Ore solution chemistry V. Solubilities of chalcopyrite and chalcocite assemblages in hydrothermal solutions at 250° to 350°C: Econ. Geol., v. 71, p. 772–794.
Donaldson, I. G., 1968, The flow of steam water mixtures through permeable beds: A simple simulation of a natural undisturbed hydrothermal region: New Zealand Jour. Sci., v. 11, p. 3–23.
—— 1962, Temperature gradients in the upper layers of the earth's crust due to convective water flows: Jour. Geophys. Research, v. 67, p. 3449–3459.
Elder, J. W., 1965, Physical processes in geothermal areas, *in* Lee, W. H. K., ed., Terrestial heat flow, Geophys. Mon. Ser. 8: Baltimore, American Geophysical Union, p. 211–239.
—— 1966, Heat and mass transfer in the earth: hydrothermal systems: New Zealand Dept. Sci. Indus. Research Bull. 169, p. 1–115.
—— 1967, Steady free convection in a porous media: Jour. Fluid Mechanics, v. 27, p. 29–48.
Fyfe, W. S., 1974, Heats of chemical reactions and submarine heat production: Royal Astron. Soc. Geophys. Jour., v. 37, p. 213–215.
Fyfe, W. S., and Henley, R. S., 1973, Some thoughts on chemical transport processes, with particular reference to gold: Minerals Sci. Eng. v. 5, p. 295–303.
Henley, R. W., 1973, Some fluid dynamics and ore genesis: Inst. Mining Metallurgy Trans., v. 82B, p. 1–8.
Holland, H. D., 1972, Granites, solutions and base metal deposits: Econ. Geol. v. 67, p. 281–301.
Holst, P. H., and Aziz, K., 1972, Transient three-dimensional natural convection in confined porous media: Internat. Jour. Heat Mass Transfer, v. 15, p. 73–90.
James, A. H., 1971, Hypothetical diagrams of several porphyry copper deposits: Econ. Geol., v. 66, p. 43–47.
Keenan, J. H., Keyes, F. G., Hill, P. G., and Moore, J. G., 1969, Steam tables: New York, John Wiley & Sons, Inc., p. 162.
Kilinc, J. A., and Burnham, C. W., 1972, Partitioning of chloride between a silicate melt and coexisting aqueous phase from 2 to 8 kilobars: Econ. Geol., v. 67, p. 231–235.
Lapwood, E. R., 1948, Convection of a fluid in a porous medium: Cambridge Philos. Soc. Proc., v. 44, p. 508–521.
Lindgren, W., 1907, The relation of ore deposition to physical conditions: Econ. Geol., v. 2, p. 105–127.
Lister, C. R. B., 1974, On the penetration of water into hot rock: Royal Astron. Soc. Geophys. Jour., v. 39, p. 465–509.
Lovering, T. S., 1935, Theory of heat conduction applied to geological problems: Geol. Soc. America Bull., v. 46, p. 69–94.
Lowell, J. D., and Guilbert, J. M., 1970, Lateral and vertical alteration-mineralization zoning in porphyry ore deposits: Econ. Geol., v. 65, p. 373–408.
Mercer, J. W., Pinder, G. F., and Donaldson, I. G., 1975, A galerkin-finite element analysis of the hydrothermal system at Wairakei, New Zealand: Jour. Geophys. Research, v. 80, p. 2608–2621.
Moore, W. J., and Nash, J. J., 1974, Alteration and fluid inclusion studies of the porphyry copper ore body at Bingham, Utah: Econ. Geol., v. 69, p. 631–645.
Muskat, M., 1937, The flow of homogeneous fluids through porous media: New York, McGraw Hill, p. 763.
Norton, D. L., 1972, Concepts relating anhydrite deposition to solution flow in hydrothermal systems: Internat. Geol. Cong., 24th, Montreal 1972, Sec 10, p. 237–244.
Norton, D. L., and Cathles, L. M., in press, Thermal aspects of ore deposition, in Barnes, H. L., ed., Geochemistry of hydrothermal ore deposits, 2nd ed.: New York, Holt, Rinehart and Winston.
Ohmoto, H., and Rye, R. O., 1974, Hydrogen and oxygen isotopic compositions of fluid inclusions in the Kuroko deposits, Japan: Econ. Geol., v. 69, p. 947–953.
Palm, E., Weber, J., and Kuernvold, O., 1972, On steady state convection in porous medium: Jour. Fluid Mechanics, v. 54, p. 153–161.
Peaceman, D. W., and Rachford, H. H., 1955, The numerical solution of parabolic and elliptic differential equations: Jour. Soc. Indus. Appl. Math., v. 3, p. 28–41.
Phillips, W. J., 1973, Mechanical effects of retrograde boiling and its probable importance in the formation of some porphyry ore deposits: Inst. Mining Metallurgy Trans., v. 82B, p. 90–98.
Ribando, R. J., Torrance, K. E., and Turcotte, D. L., 1976, Numerical models for hydrothermal circulation in the oceanic crust: Jour. Geophys. Research, v. 81, p. 3007–3012.
Roedder, E., 1971, Fluid inclusion studies on the porphyry-type ore deposits at Bingham, Utah, Butte, Montana, and Climax, Colorado: Econ. Geol., v. 66, p. 98–120.
Rubin, H., 1973, Effect of solute dispersion on thermal convection in a porous medium layer: Water Resources Research, v. 9, p. 968–973.
Schmidt, E., 1969, Properties of water and steam in SI-units: New York, Springer-Verlag, p. 205.
Sheppard, S. M. F., Nielsen, R. L., and Taylor, H. P., Jr., 1971, Hydrogen and oxygen isotope ratios in minerals from porphyry copper deposits: Econ. Geol., v. 66, p. 515–542.
Snow, D. J., 1968, Rock fracture spacings, openings and porosities. Am. Soc. Civil Eng. Jour. Soil Mech. Found., v. SM1, p. 73–91.
Sourirajan, S., and Kennedy, G. C., 1962, The system H_2O-NaCl at elevated temperatures and pressures: Am. Jour. Sci., v. 260, p. 115–141.
Taylor, H. P., 1971, Oxygen isotope evidence for large-scale interaction between meteoric ground waters and tertiary grandodiorite intrusions, western Cascada Range, Oregon: Jour. Geophys. Research, v. 76, p. 7855–7874.
Torrance, K. E., 1968, Comparison of finite difference computations of natural convection: [U. S.] Natl. Bur. Standards Jour. Research, v. 72B, p. 281–301.
Weast, R. C., 1971, Handbook of chemistry and physics, Cleveland, The Chemical Rubber Co., p. F36.
White, D. E., Muffler, L. J. P., and Truesdell, A. H., 1971, Vapor-dominated hydrothermal systems compared with hot-water systems: Econ. Geol., v. 66, p. 75–97.
Whitney, J. A., 1975, Vapor generation in a quartz monzonite magma: A synthetic model with application to porphyry copper deposits: Econ. Geol., v. 70, p. 346–358.
Wooding, R. A., 1957, Steady state free thermal convection of liquid in a saturated permeable medium: Jour. Fluid Mechanics, v. 2, p. 273–285.

APPENDIX I

Parameter	Definition	Units	Value used	Comments
c_f	Heat capacity of water	cal/gm-°C		Variable, see $\mathcal{H}$
c_m	Heat capacity of the fluid saturated rock formation (media)	cal/gm-°C	0.2	See Carslaw and Jaeger (1959, appendix VI)
d	Effective fracture aperture	cm	<0.03	
g_0	Gravitational field strength	cm/sec²	980	
H	Depth extent of system—i.e., depth to which fluid flow is permitted	cm	5.0 km	
$\mathcal{H}$	Enthalpy of water	cal/gm	Pure water values; see Figure 1c	
j_T	Diffusional flux of heat	calories/cm²-sec	Computed	Wairakei's regional average over 2,500 km² is 50 μ cal/cm²-sec with heat flow in the more intense parts of each local area ~10,000 μcal/cm²-sec (Elder, 1965)
k′	Permeability of a porous fractured media to fluid flow	cm²	0.05–0.5 millidarcies	10^{-11} cm² = 1 md
K_m	Thermal conductivity of water saturated rock	cal/cm-sec-°C	6×10^{-3}	Donaldson (1968) picks mean value of 3×10^{-3} cal/cm-sec-°C
p	Hydrostatic pressure	dynes/cm²		
p_0	Component of p that depends only on depth (z)			
q	Darcy fluid mass flux	g/cm²-sec		Wairakei's 4×10^5 gm/sec over area of 13 km² indicates q = 94 g/cm²-yr (Donaldson, 1968)
R	Heat of reactions that alter intrusive	cal/g-°C	0.0666	See Norton and Cathles (in press) and discussion of eq. (3) in text
T	Temperature of water saturated rock or fluid that flows through it	°C		Water and rock assumed always at (essentially) the same temperature
v	Fluid velocity	cm/sec		
V	Darcy velocity	cm/sec		$V = v\phi_f$
α	Coefficient of thermal expansion	°C^{-1}	10^{-3}	
γ	Pseudoheat capacity	cal/g-°C	Figure 3b	Ratio of enthalpy to temperature at each grid location at the previous timestep or the average value between timesteps
ν	Kinematic viscosity	cm²-sec^{-1}	Pure water values, see Figure 1c	
ρ	Fluid density gm/cm³		Pure water values, see Figure 1a	
ρ_m	Density of the fluid saturated rock formation	g/cm³	2.7	
ρ_0	Fluid density variations that are a function of depth (z) only	g/cm³		
Φ	Total formation porosity including both flow fracture porosity and pore porosity in the impermeable matrix blocks between flow fractures	Dimensionless	$2\text{–}4 \times 10^{-2}$	
Φ_f	Flow channel or fracture porosity in the direction of flow	Dimensionless	$\sim 10^{-3}$	
$\underline{\psi}$	Vector stream function describing fluid flow	cm²/sec		$\underline{\nabla} \times \underline{\psi} = \underline{q}$
ψ_x	x component of the vector stream function (appropriate for 2 dimensional flow)	cm²/sec		$\underline{\nabla} \times \psi_x \hat{x} = \underline{q}$
$\bar{\psi}$	Dimensionless stream function			$\bar{\psi} = \psi \mathcal{H}^*/K_m T^*$; $\mathcal{H}^* = 1$ cal/g, $T^* = 1$°C